VIRGINIA WATER RESOURCES RESEARCH CENTER

ANALYSIS OF SINKHOLE SUSCEPTIBILITY AND KARST DISTRIBUTION IN THE NORTHERN SHENANDOAH VALLEY, VIRGINIA: IMPLICATIONS FOR LOW IMPACT DEVELOPMENT (LID) SITE SUITABILITY MODELS

SPECIAL REPORT

Virginia Tech

VIRGINIA POLYTECHNIC INSTITUTE AND STATE UNIVERSITY
BLACKSBURG, VIRGINIA
2006

This report is available online. Hard copies may be obtained from the
Virginia Water Resources Research Center for a small fee.
210 Cheatham Hall
Blacksburg, VA 24061
(540) 231-5624
FAX: (540) 231-6673
E-mail: water@vt.edu
Web address: http://www.vwrrc.vt.edu

Stephen Schoenholtz, Director

ANALYSIS OF SINKHOLE SUSCEPTIBILITY AND KARST DISTRIBUTION IN THE NORTHERN SHENANDOAH VALLEY, VIRGINIA: IMPLICATIONS FOR LOW IMPACT DEVELOPMENT (LID) SITE SUITABILITY MODELS

by

Sara E. Hyland
Lisa M. Kennedy
Tamim Younos
Shane Parson

Virginia Water Resources Research Center
210 Cheatham Hall
Virginia Tech
Blacksburg, Virginia 24061-0444

August 2006

VWRRC Special Report SR31-2006

SUMMARY

Increased stormwater runoff due to urban development in the northern Shenandoah Valley (NSV) region of Virginia has prompted local officials and representatives to consider Low Impact Development (LID) as a stormwater management technique. LID is based on infiltrating stormwater runoff at the source through practices such as bioretention, rain gardens, and grass swales. The karst terrain that underlies the Shenandoah Valley presents a major barrier to the use of LID. Infiltration of surface runoff in karst landscapes may threaten groundwater quality and the stability of the bedrock. In 2004 the Center for Geospatial Information Technology (CGIT) at Virginia Tech developed an LID site suitability model for the NSV region incorporating karst as a key component in distinguishing unsuitable from suitable conditions for LID. But, due to the difficulty of mapping karst, the karst layer used in the site suitability model is very coarse in resolution, based primarily on carbonate versus non-carbonate rock.

This study uses a 1:24,000 scale sinkhole map derived from sinkhole boundaries identified by geologist David Hubbard (1984) of the Virginia Department of Mines and Minerals (DMME) to develop a more detailed karst map for a sub-watershed of the NSV region. The analysis uses geospatial techniques to determine the relationship between sinkhole distribution and four major landscape factors: bedrock type, soil depth to bedrock, proximity to geologic faults, and proximity to surface streams. The analysis identified three major trends in sinkhole occurrence: (1) sinkholes are more abundant in relatively pure carbonate rocks of Ordivician age; (2) sinkhole occurrence increases with proximity to fault lines; and (3) sinkholes are sparse near streams, most abundant 600 to 1400 feet away from surface streams. Based on these findings a sinkhole susceptibility index was produced using weighted overlay analysis in ArcGIS. The

sinkhole susceptibility index provides a more detailed karst layer for the LID site suitability maps and can be used by the NSV region as a predictive tool for future sinkhole occurrence.

ACKNOWLEDGEMENTS

The authors would like to acknowledge several people for their support and contributions towards this work:

David Kramar, for his invaluable advice on what statistical analyses to choose, and for always being available to discuss complex concepts at great lengths and detail over email or phone.

David Hubbard, geologist for the Virginia Department Mines and Minerals, for his helpful discussion on karst mapping, allowing to use his sinkhole data in my research, and initiating the idea to overlay sinkholes with geologic bedrock formations.

Wil Orndorff, Karst Protection Coordinator of the Virginia Division of Natural Heritage, for his karst expertise and helpful comments.

Jim Campbell, professor of Geography, for his valuable advising on statistics and geomorphology.

TABLE OF CONTENTS

ABSTRACT ..... **Error! Bookmark not defined.**
ACKNOWLEDGEMENTS 4
LIST OF TABLES 6
LIST OF FIGURES 7
INTRODUCTION 8
Background 9
The original karst map 14
The need for studies of sinkhole distribution 16
OBJECTIVE 18
METHODOLOGY 18
Study Area 18
Data acquisition and preparation 19
Analysis of *categorical data* 22
Analysis of c*ontinuous data* 24
Individual and aggregate susceptibility index 25
RESULTS 26
Categorical variables 26
Continuous variables 28
Criteria weighting and susceptibility indices 29
DISCUSSION 30
Geologic bedrock 30
Soil depth to bedrock 32
Proximity to fault lines 33
Proximity to surface streams 34
Sinkhole susceptibility index 35
CONCLUSION AND APPLICATIONS 37
Implications for LID site suitability 38
Recommendations for future work 38
LITERATURE CITED 41
TABLES 44
FIGURES 60

LIST OF TABLES

Table 1. LID practices by mapping category. 44
Table 2. Data sources 45
Table 3. Geologic bedrock 46
Table 4. Methods for determining sinkhole susceptibility rankings for bedrock types. 48
Table 5. Chi-square results of Kruskal-Wallis test on bedrock type..... 49
Table 6. Mean ranks produced by the Kruskal-Wallis test 50
Table 7. Results of cross tabulation analysis for bedrock type. 51
Table 8. Odds ratio results for sinkhole occurrence in bedrock type..... 52
Table 9. Coefficients of the regression line for continuous variables. 53
Table 10. Results of the ANOVA for the continuous variables. 54
Table 11. Regression model summaries for continuous variables. 55
Table 12. Sinkhole occurrences and expected occurrences for continuous variables..... 56
Table 13. Geologic bedrock sinkhole susceptibility rankings..... 54
Table 14. Sinkhole susceptibility rankings for distance from fault intervals. 55
Table 15. Sinkhole susceptibility rankings for distance from stream intervals. 56
Table 16. Sinkhole susceptibility index. 57
Table 17. Attributes of sinkhole containing bedrocks that increase sinkhole susceptibility..... 58
Table 18. Associating LID suitability with sinkhole susceptibility. 59

LIST OF FIGURES

Figure 1. Map of the Northern Shenandoah Valley (NSV) region of VA 60
Figure 2. LID site suitability map 61
Figure 3. Karst map of the NSV region. 62
Figure 4. Map of study area 63
Figure 5. Method for creating a GIS data layer for the 1:24,000 scale sinkholes..... 64
Figure 6. Geologic bedrock layer for carbonate rocks. 65
Figure 7. Method for assigning a distance to fault interval to each sinkhole 66
Figure 8. Distance to fault line intervals data layer 67
Figure 9. Distance to surface stream intervals data layer……. 68
Figure 10. Methods for determining sinkhole morphology for each bedrock type 69
Figure 11. Transect map..... 70
Figure 12. Histogram and P-P plot for distance to fault data……...71
Figure 13. Histogram and P-P plot for distance to surface stream data……..... 71
Figure 14. Sinkholes versus distance to fault intervals……72
Figure 15. Sinkholes versus distance to stream intervals…….....72
Figure 16. Number of occurred and expected sinkholes (fault data)…..……..73
Figure 17. Number of occurred and expected sinkholes (stream data)…….. 73
Figure 18. Sinkhole susceptibility index……..... 74
Figure 19. Map of anomalies in distance to fault line regression model…… 75

INTRODUCTION

Communities in regions dominated by limestone and dolomitic bedrock are particularly vulnerable to the environmental degradation that accompanies land use change and urbanization, especially those that rely on underground aquifers for water supply. Growing environmental problems, especially concerning water quality, along with technological advances in Geographic Information Systems (GIS), have given rise to increased efforts by researchers, engineers, and planners to better understand the spatial distribution of karst features that characterize these regions. Major karst mapping initiatives have been launched in south-central Texas (Stone and Schindel 2002), Mower County, Minnesota (Green et al. 2002), and in the Suwannee river basin of Florida (Denizman 2003). GIS applications enable researchers to objectively identify the conditions that trigger karst hazards. However, karst formations develop in very specific ways that are influenced by the unique local conditions of the area (Waltham and Fookes 2003). Local climate, geology, and urban development all affect the evolution of karst formations.

There have been few quantitative investigations of the complex karst features that dominate the Northern Shenandoah Valley (NSV) region of Virginia. The NSV region, northwest of Washington DC, is a predominantly rural area that has experienced rapid urban growth along Interstate 81. Urbanization, in conjunction with recent droughts, has prompted communities to express concern over water availability and water quality conditions. As part of a project funded by a Chesapeake Bay Small Watershed Grant through the National Fish and Wildlife Foundation, the Northern Shenandoah Valley Regional Commission (NSVRC) tasked the Center for Geospatial Information Technology (CGIT) at Virginia Tech with developing a Low Impact Development (LID) site suitability model for the region using GIS. LID is a

strategy designed to decrease surface water runoff at the source by increasing infiltration, thereby preserving water quantity and water quality. CGIT recognized that the objectives of LID could be compromised by the underlying karst in the region and could even lead to lower water quality (more pollution) as well as bedrock instability if LID was implemented over a karstic landscape. The only karst map available to CGIT was a 1:250,000 scale map produced by the Virginia Division of Mineral Resources (DMME), which was based primarily on carbonate versus non-carbonate rock. Due to its lack of detail, the map does little to inform the region about why karst formations occur in some areas and not others.

This thesis is a part of the larger LID project led by CGIT and is aimed at providing a better understanding of the spatial distribution of karst features in the NSV region. The objective of my study was to use a GIS to develop a more detailed karst map for a sub-watershed of the NSV region to assist in future planning initiatives. Sinkholes are easily visible surface features, which indicate the presence of karst terrain. The analysis used geospatial techniques to determine the relationship between sinkhole distribution and four major landscape factors: bedrock type, soil depth to bedrock, proximity to geologic faults, and proximity to surface streams. The results of this research fill a gap in the karst literature by providing a landscape scale analysis of karst formations local to Virginia, and a higher resolution karst map to be incorporated into development design strategies such as LID.

Background

Karst terrain is a geological formation that results from the interaction of soluble rocks with acidic water. Soluble rocks include limestone, dolomite, and gypsum. Of this group the

carbonate rocks, limestone and dolomite, dominate much of the geology in the lowlands of the NSV region of Virginia (Figure 1).

Karst processes work similarly in carbonate rocks in many regions. As rainwater passes through soil horizons, the water absorbs carbon dioxide and becomes increasingly acidic. As the acidic water percolates through the fractures and fissures that are characteristic of carbonate rocks, these openings become enlarged through dissolution, and water transport increases. Gradually karst formations such as conduits, caves, sinkholes, and aquifers develop in the area. The resulting underground and surface structure has been described by Zwahlen and Doerfliger (1997) as "a network of connected channels reaching outlets which drain or recharge a volume of weakly permeable fissured or fractured rock." The complex and unique drainage systems that occur in karst landscapes warrant careful consideration when planning for development.

One major threat to water quality and availability in urban areas is increased stormwater runoff due to increased impervious surfaces; this problem escalates dramatically in karst landscapes. Karst terrains are especially sensitive to environmental stresses and such problems are compounded in areas experiencing increased land use, particularly through urbanization (Kastning and Kastning 1997). Kastning and Kastning (1997) list four typical environmental problems associated with urban development in karst areas: (1) instability and collapse of the ground surface, (2) erosion or sedimentation of sinkholes, (3) flooding of sinkholes, and (4) contamination of groundwater. These problems are directly associated with the increased volume and rate at which surface water runs off impermeable urban structures such as roofs, sidewalks, streets, and parking lots. The subsequent rapid movement of polluted surface water through the underground conduits of karst formations contributes to sharp increases in

groundwater pollution. Additionally, the increased volume of surface runoff in urban areas can accelerate dissolution of openings in the karst formations and thus cause instability of the bedrock.

One of the more visible karst formations indicative of bedrock instability are sinkholes. Sinkholes can be induced through natural or human activity related causes. Sinkholes that occur naturally usually form by the slow downward dissolution of carbonate rock or through bedrock collapse in areas that overlie caverns (Langer 2001). Human induced sinkholes can be triggered by simple alterations in the local hydrology, e.g. from landscaping a yard. Inadequate drainage along highways and increased runoff from pavements can also be sources of sinkhole development (Hubbard 2003). Most human induced sinkholes are caused by the lowering of water tables below the rock/soil interface (Langer 2001). Dewatering an underground limestone quarry for the purposes of water supply can lower water tables. For example, in 1949 increased pumping of a quarry in Hershey Valley, Pennsylvania created nearly 100 sinkholes within three months of the increased pumping (Langer 2001). Sinkhole development stopped once the pumping was halted and the water table level returned to normal (Langer 2001).

The most catastrophic sinkhole events are those that occur instantaneously; these can even result in loss of life (Waltham and Fookes 2003). These events occur when arches of cohesive soils, developed over growing voids caused by dissolution, finally collapse (Hubbard 2003; Waltham and Fookes 2003). More typical hazards include the degradation of buildings and other structures and road networks.

In response to the environmental problems associated with karst, much of the karst research is dedicated to addressing the impacts of urban development on karst landscapes. Veni

(1999) studied the effects of impervious surfaces on karst areas and found that adverse environmental impacts significantly increase when impervious cover exceeds 15% of a surface watershed. Stephenson et al. (1999) studied the impacts of highway stormwater runoff in karst areas in Knoxville, Tennessee and found that contaminant load in a karst formation is more closely related to the volume of runoff than to the contaminant concentration. Currens (2002) compared water quality in agricultural watersheds characterized by karst before and after the implementation of some typical Best Management Practicies (BMPs). Currens concluded that the BMPs did little to improve water quality and suggested that future BMPs in karst areas should emphasize buffers around sinkholes.

It is clear from the literature that urban development can have costly negative effects on karst water quality. Much of the past environmental destruction associated with karst can be linked to a pervasive lack of understanding among people living in karst regions about karst processes (Kastning and Kastning 1997). Waltham and Fookes (2003) postulated that karst problems around the globe are exacerbated by insufficient understanding of karst by engineers. In response, many researchers (Zwahlen and Doerfliger 1997; Kastning and Kastning 1997; Green et al. 2002; Denizman 2003; and Waltham and Fookes 2003) adamantly assert that it is essential to understand the hydrologic network of the karst terrain when implementing urban development design strategies. Not only is it important to preserve fragile karst features, it may also be necessary to avoid some of the current stormwater management techniques that promote infiltration of surface runoff. One such technique is Low Impact Development (LID).

LID strategies such as rain gardens, bioretention, and grass swales promote infiltration at the source in an effort to preserve water quality and water quantity. LID has been widely

recognized as more sustainable and economical than conventional approaches to water management. Karst terrain, however, poses a major challenge to LID. Water transported through underground karst rocks does not benefit from the natural filtration of contaminants that occurs in most non-karst landscapes (Kastning and Kastning 1997). In addition, relatively small changes to surface features, such as those that occur during landscaping, can alter run-off patterns in a way that triggers karst hazards, for example causing new sinkholes to appear (Hubbard 2003). The infiltrated water from LID techniques may collapse the land over sinkholes, enlarge conduits, or otherwise alter the hydrologic function of the groundwater karst aquifers, leading to reduced groundwater quality.

The advent of LID, the continuing pressure to develop karst regions, and the general lack of understanding of karst by the public greatly increases the importance of understanding how LID and development will affect groundwater transport and quality in the karstic NSV region of Virginia. The NSV region extends from Shenandoah and Page counties to Frederick and Clarke counties, including Warren county and the city of Winchester. These predominantly rural counties are expected to face rapid urbanization as the Washington, DC commuter corridor continues to expand (Orndorff and Harlow 2002). This rapid urban growth, in conjunction with recent droughts, has caused regional and local planners concern over water availability and water quality conditions. The NSV region is eager to implement sustainable development strategies such as LID in order to protect their resources.

In 2004 the Center for Geospatial Information Technology (CGIT) at Virginia Tech used a GIS to complete regional scale site suitability maps for LID in the NSV region. With advancements in GIS technology and increased availability of GIS data layers in Virginia, this

task was successfully completed within months. First, a total of fifteen LID practices were identified as appropriate practices for the NSV region (Table 1). Other practices may be appropriate but were outside the scope of the project. In order to simplify the suitability requirements for each LID practice, the practices were grouped into three categories: *infiltration based with specific slope requirement, infiltration based with no specific slope requirement,* and *non-infiltration based* (Table 1). Each category required an individual LID site suitability map. To the benefit of the NSV region, communities now have access to regional maps that identify areas of high, moderate, low, and very low suitability for different types of LID practices (Figure 2). The maps take into account zoning, soil infiltration, soil depth to bedrock, slope, and the presence of karst. They are useful for providing general guidelines for implementation of LID in broad geographic areas. However, when implementing LID in areas of mixed suitability it is important to conduct more site specific analyses.

Uncertainty is inherent in all maps and is likely associated with each GIS layer incorporated in the regional scale LID site suitability map. However, the karst data layer presents the most uncertainty and yet demands greater accuracy for four reasons: (1) the current karst map used in the GIS provides low resolution data because it is at the 1:250,000 scale, (2) karst is very difficult and time consuming to map, which may have negatively affected the accuracy of the data, (3) karst terrain poses the most significant challenge to LID for the NSV region, and (4) water transport and other aspects of karst terrain are not well understood by planners and engineers.

The original karst map

The karst data layer is based on the most comprehensive karst mapping project completed in Virginia; the mapping was done by the DMME between 1980 and 1988. Most of the mapping was completed by David Hubbard, a Geologist Specialist at DMME, who located sinkholes through stereoscopic viewing of panchromatic aerial photography and plotted them on 1:24,000 scale topographic maps (Hubbard 2001). Hubbard primarily relied on these remote sensing techniques, but also performed some field checking where sinkhole locations were questionable. The final karst terrain boundaries on the map are based on the sinkhole locations and geologic maps of carbonate rocks, also developed by the DMME. The presence of carbonate rock does not guarantee karst formation, but increases its likelihood. Finally, the karst boundaries were reduced in size and transferred to a 1:250,000 scale map (Hubbard 2001).

In order to prepare DMME's karst map for the LID site suitability maps, the karst map was first scanned and geo-referenced to the Virginia North SPCS, NAD83 projection. The karst boundaries were digitized using ArcMap. Karst polygons were assigned a very low suitability ranking and the non-karst areas were assigned a high suitability ranking. The resulting suitability map is useful in that it identifies the areas that are not characteristic of karst and therefore safe for implementing LID. On the other hand, the areas that are characteristic of karst formations are large and expand across some of the highly developed areas of the NSV region including Interstate 81, the city of Winchester, and the towns of Staunton and Woodstock (Figure 3). The pressure to continue to develop in these areas is high; any LID map that completely eliminates them is practically useless in terms of planning and management.

Karst terrain is a very difficult to map. Sinkholes are the most common karst features mapped because they are an indicator of bedrock dissolution, and they can be recognized on

topographic maps or through remote sensing techniques (Shofner and Mills 2001; Hubbard 2003). Kastning and Kastning (1997) assert that "sinkholes are perhaps the single landform most useful in mapping the extent and type of karst." Kastning and Kastning (1997) also warn that field-checking is the only truly reliable way to locate all of the sinkholes in any area. However, field mapping of sinkholes in large areas is not always possible due to time constraints. Hubbard (2003) estimates that field mapping of sinkholes for a 1:24,000 scale map can take four to ten times as long as to map the geology at the same scale. As a result, when researchers map a large area they are often limited to mapping at small scales using data sources other than fieldwork. Hubbard (2002) noted that karst maps at small scales are useful because they display the relative range of sinkhole development. On the other hand, he emphasizes that the scale and resolution of the map make it inherently problematic to use for site-specific management plans. He warns that karst landscapes with high sinkhole densities are often not well suited for intense development even when it is carefully planned.

The need for studies of sinkhole distribution

There is a need to develop a more detailed version of Hubbard's karst map in a sub-watershed of the North Fork Shenandoah watershed by identifying and ranking factors that control the morphometry of mapped sinkhole formations. Morphometry is defined by Bates and Jackson (1987) as the "measurement and mathematical analysis of the configuration of the earth's surface and the shape and dimensions of its landforms." Morphometric analysis provides an objective and quantitative analysis of karst landforms. It involves measurement of sinkhole density, sinkhole coverage, and sinkhole shape including width, length, depth, and orientation, and (Denizman 2003). The environmental conditions most commonly thought to control

sinkhole morphometry are the underlying geology, including bedrock, fractures and faults, soil depth to bedrock, and local hydrology (Hack 1965; Brezinski, Reger, and Baum 2003; Gao, Alexander, and Tipping 2002; Green et al. 2002; Hubbard 2003).

The most comprehensive study of the landscape formations of the NSV region was conducted by geologist John Hack (1965) of the United States Geological Survey in his report on the geomorphology of the Shenandoah Valley. Hack agrees with the common theory in karst literature that the character of the bedrock is one of the most important factors controlling sinkhole distribution. In his report Hack examined sinkholes in the Shenandoah Valley that were identified by aerial photography. Hack found sinkholes were most abundant in carbonate rocks of middle Ordovician age where there was usually little to no residuum mantle present. He noted that sinkholes commonly occur in clusters and cited examples of sinkhole clusters that most likely relate to the presence of synclinal faults. His work also showed correlations between sinkhole distribution and surface streams. In carbonate rock areas where there are no streams entering the valley from non-carbonate rock areas, Hack found sinkhole formations lacking. He also postulated that sinks are more abundant along larger streams than smaller streams for three reasons: (1) the heavy inflow of groundwater to the streams; (2) the steepening of the groundwater gradient near large entrenched streams; and (3) the fact that many smaller streams enter the carbonate rock from the mountains and are low in dissolved solids and alkalinity. Hack also observed that sinkholes were not located immediately adjacent to streams and rather occurred at some distance a way. He suggested that this sinkhole pattern related to the circulating of groundwater also occurring at some distance a way from the main streams.

Hack's analysis provides key insight into the local sinkhole morphology of the Shenandoah Valley. He drew conclusions about sinkhole occurrence in relation to the characteristics of bedrock and the presence of geologic faults and surface streams. By using another dataset of sinkholes provided by geologist Dave Hubbard (2001), this study can serve to affirm or reject some of Hack's theories.

The unquestionable pressure to continue development of the Shenandoah Valley requires an effort to produce a more detailed large-scale (localized) karst map. Planners and communities can use the map to increase their understanding of karst and their awareness of its hazards. Analysis of karst morphology at the sub-watershed scale helps to identify the environmental conditions that enable development of karst formations in the Shenandoah Valley.

OBJECTIVE

The objective of this study is to produce a map that identifies sinkhole susceptibility across the landscape. A map based on a susceptibility range (e.g. categories of susceptibility) versus a Boolean classification model of karst will make the LID maps for this area more useful and more robust. The sinkhole susceptibility index provides a more accurate, detailed karst layer for the LID site suitability maps and will help communities in the NSV region predict the future development of sinkholes, which create physical and environmental hazards.

METHODOLOGY

Study Area

The study area (Figure 4) is a sub-watershed of the North Fork Shenandoah River in Shenandoah County. It includes 22,349 hectares and the centroid of the study area is located at 78º30'54" latitude and 38º54'9" longitude. It is representative of the NSV region because it is intersected by Interstate 81 and includes the town of Woodstock. Woodstock has experienced rapid growth in the last decade primarily due to its close proximity to Interstate 81 and the entrance to Interstate 66, which serves as a corridor to the Washington D.C. metropolitan area. This study is limited to the geographic area already designated as karst according to DMME's 1:250,000 scale karst map (Figure 3), in which there are 339 sinkholes identified by Hubbard (2001).

This study analyzes sinkhole distribution in relation to four relevant criteria: bedrock type, soil depth to bedrock, distance to geologic fault lines, and distance to surface streams. To develop a sinkhole susceptibility index, I followed three major steps, which were adapted from a study by Chen et al. (2001):

1. determine standardized values and weights for each of the four criteria based on existing literature and statistical methods (intra-attribute comparisons);
2. generate individual susceptibility maps for each of the criteria based on previous studies and statistical methods (inter-attribute comparisons);
3. derive an aggregated susceptibility map based on individual criteria maps.

Data acquisition and preparation

I used five primary data sources for this analysis (Table 2). I scanned, geo-referenced, and digitized the sources for the karst boundary layer, sinkhole layer, and bedrock layer into

vector based shapefiles using ArcMap. The bedrock layer includes 13 distinct formations (Table 3, Figure 6). The bedrock data layer does not include terrace deposits or alluvium that overlay much of the geology because it is unlikely that they play a role in karst development (Orndorff, personal communication 2005). If any relationship does appear to exist between these deposits and the presence of sinkholes, it is likely a common-cause relationship. In other words, sinkholes are more likely to form near the river where the karst systems have an outlet for sediment and a higher hydraulic gradient. Terrace deposits are also more likely to be found near the river by simple virtue of their origin (Orndorff, personal communication 2005).

The soil depth to bedrock data layer is derived from the MUAGGAT (Mapunit Aggregated Attribute Table) table provided in the Soil Survey Geographic (SSURGO) database. Using the "relate" tool in ArcGIS, I linked the MUAGGAT table to the shapefile that spatially delineates soils based on mapunit ID. I added a soil depth to bedrock field to the shapefile. By updating the "relate" between the tables repeatedly and using selection tools, I manually entered the soil depth to bedrock class for each soil mapunit. Finally, I adjusted the symbology of the shapefile to display soil unit according to soil depth class.

The steps used to produce the distance to fault line data from the digitized fault lines are outlined in Figure 7. The final distance to fault data layer (Figure 8) is a series of polygons that extend outward at equal intervals of 250 feet from the faults. In other words, the outer boundary of nearest polygon, or Interval 1, is 250 feet from the nearest fault line and the outer boundary of Interval 30 is 7500 (250x30) feet from the nearest fault line. I selected all the sinkholes that were located in each interval and populated the corresponding interval numbers into a distance to fault field of the sinkhole attribute table.

In preparing the distance to surface stream data, I first used the spatial analyst tool to create a stream network data layer from the DEM with a maximum of 2500 cells. I then converted the stream network raster layer to a vector based layer. I used the same methods to populate a distance to surface stream field in the sinkhole attribute table as in the distance to fault line field. The final distance to stream shapefile (Figure 9) contains 25 equal intervals of 100 feet.

Data analysis

I used spatial overlay analysis in ArcGIS and statistical techniques in Statistical Package for the Social Sciences (SPSS) to determine weights that express the importance of each criterion relative to the others in terms of sinkhole susceptibility. The results of the statistical analysis and the results of other studies in the karst literature (e.g. Hack 1965) helped me to determine weights for intra-attributes (among the criterion) as well as rankings for inter-attributes (within each criteria). I produced a final sinkhole susceptibility index by multiplying each criterion by the corresponding weight and then summing these products over all the criteria.

Sinkhole Susceptibility Index (SSI) = (Inter-attribute rankings $_a$) (Intra-attribute weight $_a$) + (Inter-attribute rankings $_b$) (Intra-attribute weight $_b$) + (Inter-attribute rankings $_c$) (Intra-attribute weight $_c$)

The four criteria used for this analysis fell into two distinct groups based on data scale: two were categorical and two were continuous. I used statistical analyses appropriate for each of the categories; categorical data require non-parametric methods that do not assume that the data are normally distributed, while parametric methods can be used with continuous scale data.

Analysis of *categorical data*

The categorical data included bedrock type and soil depth to bedrock data. Both these factors are frequently mentioned in the literature as being primary controls for sinkhole development. For these criteria I used a Kruskal-Wallis procedure (Sokal and Rohlf 1995) to test the null hypothesis that sinkholes have the same distribution across all classes within each criterion in terms of sinkhole density, percent of sinkhole coverage, and average sinkhole size:

Sinkhole density = sinkhole count / class area (hectares)
% sinkhole coverage = (sinkhole area within class (hectares) / class area (hectares)) 100

Using density and percent coverage estimates eliminates the bias that stems from the highly variable amount of area that each bedrock type covers. Steps used to determine sinkhole density, percent of sinkhole coverage, and average sinkhole size for the categorical criteria are described in Figure 10. These sinkhole calculations serve as dependent variables while bedrock class and soil depth to bedrock class serve as independent variables.

In order to use the Kruskal-Wallis procedure, I divided the study area into five transects of approximately equal area so that sinkhole distribution could be compared among samples (Figure 11). The transects were generated automatically using GIS. I manually altered the location of transects that intersected sinkholes so that the transect did not effect the mean sinkhole size variable. For the categorical values with significant relationships with sinkhole distribution, I used the Kruskal-Wallis significance value to help establish a weight that reflected the importance of the criterion (intra-attribute comparison).

I used a cross tabulation procedure (Upton 1978) and odds ratio statistics (Agresti 1996) to quantify the variation within the criteria (inter-attribute comparison). To perform cross

tabulations the dependent variables were classified into categories. Using SPSS, I classified the values for sinkhole density, percent of sinkhole coverage, and average sinkhole size into four categories based on equal intervals: very high, high, moderate, or low. These classifications were relative to the specific study area and would not necessarily work in other geographical areas. The cross tabulation identified classes of the independent variables that accounted for each of these categories, and indicated the variability in sinkhole distribution among the five transects.

In contrast to cross tabulation, odds ratio statistics estimate whether the probability of sinkhole occurrence is the same for all criteria classes. A typical 2x2 odds ratio table follows:

	X^-	X^+	
Y^-	a	b	a + b
Y^+	c	d	c + d
	a + c	b + d	

The odds ratio = *(a/b)/(c/d)*. The odds ratio is the ratio of two odds whereas the relative risk is a ratio of two probabilities. The relative risk (RR) for the event X- would be given by the formula:

$$RR = \frac{a/(a + b)}{c/(c + d)}$$

Relative risk is a more direct method for comparing the two probabilities. The relative risk estimates that X^- is likely to contain *n* times the number of sinkholes as Y^+.

Odds ratio statistics require two dependent variables: sinkholes and non-sinkholes. To generate non-sinkholes I used an ArcGIS extension titled Hawth's Tools acquired from

http://spatialecology.com. Hawth's Tools can generate random points throughout the study area, and at the same time prevent points from generating where there are sinkholes. The result was a shapefile of 339 random points (equal to the number of sinkholes) that represents points where no sinkhole was previously identified. I used selection tools in ArcGIS to identify the classes of the independent variables that overlay each sinkhole and random point. The class labels were populated into corresponding fields of the sinkhole and random points attribute tables. Finally, I determined a count for each class and then created a matrix of these count values in a spreadsheet to calculate the odds ratio statistics for every class.

I created a similarly structured matrix to compute relative risk. Evaluation of both the cross tabulation and odds ratio results helped to determine rankings for the inter-attribute criteria and thus generate individual sinkhole susceptibility maps for both of the categorical criteria.

Analysis of c*ontinuous data*

The continuous data included distance from geologic fault lines and distance from surface streams. Associations between fault lines and karst formations have been documented in the literature (Hack 1965). Proximity to surface streams relates to hydraulic gradient which is considered to be a primary control in sinkhole distribution (Hack 1965).

To quantify the relationship between sinkhole occurrence and the continuous data criteria, I used linear regression analysis. In the linear regression, the centers of the sinkholes served as the dependent variables and distance to the continuous variables served as the independent variables.

I verified that the data were normally distributed using SPSS by applying a histogram and normal probability plot (P-P) to the residuals of the data. I calculated Cook's distance and plotted the values against leverage values to determine if there were any influential points that weighed heavily on the regression model.

The robustness of the regression model was indicated by the R-value, the multiple correlation coefficient, and the significance of the F statistic. The weights assigned to the criteria (intra-attribute comparison) were largely based on the amount of variation in sinkhole distribution that the model was able to explain (R^2). Then, the expected values as indicated by the coefficients of the regression line, as well as deviations from the regression line, contributed to the assignment of rankings for each distance interval (inter-attribute comparison), which reflected the strength of the relationship between the distance interval and sinkhole occurrence. The resulting values were used to generate individual sinkhole susceptibility maps for both of the continuous criteria.

Individual and aggregate susceptibility index

Methods for generating sinkhole susceptibility maps for the individual criteria differed between the categorical variables and the continuous variables. I multiplied the rankings for the inter-attributes of each criterion by the corresponding intra-attribute weight, and then added all the products together. The inter-attribute rankings of the categorical analyses were based on previous studies in the literature and the results of the statistical analysis. For example, Table 4 outlines the equation used to determine the individual susceptibility index for the geologic bedrock layer. The evaluation scale for each categorical criterion ranges from 0 to 1. The following equation classifies the categorical criteria into four susceptibility rankings with 1 being

the least susceptible to sinkhole development and 4 being the most susceptible to sinkhole development:

$$\frac{\text{Sum of the criteria}}{\text{Maximum rank}} (4) = \text{susceptibility index}$$

In generating individual susceptibility indices for the continuous data, I assigned rankings to particular distance intervals based on how well the data fit to the regression models. I also considered deviations form the models if the deviations could be explained by other variables or previous karst studies in the literature.

Before adding all of the individual susceptibility maps together, I converted each criteria layer from vector format to raster format. Then, I used the weighted/overlay analysis tool in ArcGIS version 9.0 to aggregate all of the criteria layers into one final sinkhole susceptibility index. I entered in the assigned weights that represented the influence of each criterion and the assigned rankings of each criterion class. The rankings were based on an evaluation scale of 1 to 8 with even numbers representing a scale of 1 to 4 and odd numbers representing the half way points between those numbers. This is a common method when using the weighted/overlay analysis tool because the tool limits the evaluation scale to whole numbers ranging from 1 to 9. Finally, I used a classification method based on natural breaks to generate a map that categorizes sinkhole susceptibility into four class: low, moderate, high, and very high susceptibility.

RESULTS

Categorical variables

The results of the Kruskal-Wallis test indicated that sinkholes do not have the same distribution across all bedrock classes in terms of sinkhole density and percent of sinkhole coverage (Table 5). Chi-square values for both the sinkhole density (13.45) and percent sinkhole coverage (14.05) exceeded the critical value (11.07, $\alpha = 0.05$, $df = 5$). These results indicated significant differences in sinkhole density and percent sinkhole coverage among the six bedrock classes in which sinkholes occur. Average sinkhole size, on the other hand, did not vary significantly among the bedrock classes (chi-square value 9.4, $df = 5$).

The mean ranks produced by the Kruskal-Wallis test (Table 6) showed the relative extent of variation in sinkhole density or percent sinkhole coverage in each bedrock class. Cross tabulation and odds ratio statistics further identified bedrock classes that were more likely to have greater impact on sinkhole distribution. The cross tabulation analysis for sinkhole density (Table 7) indicated that 50% of the 'very high' sinkhole density values fall in the New Market Limestone formation. The Conococheague formation makes up 71.4% of the 'low' sinkhole density values. The bedrock classes could be ranked in terms of descending sinkhole density based on the cross tabulation results, with the New Market Limestone and Lincolnshire formations as the top two, Conococheague at the bottom, and the Stonehenge, Beekmantown, and Edinburg formations in between.

The cross tabulation analysis for percent sinkhole coverage (Table 7) indicated that 37.5% of the 'very high' values fell in the Lincolnshire formation; 71.4% of the 'low' values occurred in the Conococheague formation. The remaining bedrock classes fell in the 'high' and 'moderate' categories.

The cross tabulation procedure also indicated how the data varied among the transects. Sinkhole density and percent of sinkhole coverage appeared least variable in the Conococheague formation because the values across all five transects fell in the 'low' category. There is considerable variation in percent sinkhole coverage in the New Market Limestone; however sinkhole density is relatively consistent with four transects displaying values in the 'very high' category and one value in the 'moderate' category.

The odds ratio statistics estimated that on average a sinkhole was 1.4 times more likely to fall in the New Market Limestone formation than any other bedrock class that contains sinkholes (Table 8). In agreement with the cross tabulation findings, the odds ratio statistics also indicated that sinkholes were least likely to develop in the Conococheague formation.

The Kruskal-Wallis test indicated no significant differences in sinkhole density, percent sinkhole coverage, or average sinkhole size across soil depth to bedrock classes, so no further statistical analyses were performed.

Continuous variables

Histograms and P-P plots of the residuals of the dependent variables verified that both the proximity to fault line data (Figure 12) and proximity to surface stream data (Figure 13) were normally distributed. Scatter plots graphically demonstrated the relationship between sinkhole occurrence and distance from fault intervals (Figure 14) and distance from surface stream intervals (Figure 15). The regression analysis and ANOVA (Tables 9, 10, and 11) showed significant relationships between both distance to faults and distance to streams, and variance in the number of sinkholes.

Sinkhole abundance was positively related to proximity to fault lines (R^2=0.60, $p<0.05$). Of 30 distance intervals, nearly 24% of the total sinkholes occur in the first 3 intervals (within 750 ft of fault lines) (Table 11). Sinkhole abundance was also positively related to proximity to surface streams (R^2=0.52, $p<0.05$).

Scatter plots of the number of occurred sinkholes overlaid by scatter plots of the number of expected number sinkholes, as predicted by the regression models, graphically indicated how well the data fit to the models (Figures 16 and 17). For the distance to fault line regression, the real values deviated from the expected values significantly in two places (Figure 16). First, according to the regression analysis, the number of sinkholes that occurred in the first distance interval (0–250ft) was well above the expected value. Second, the number of sinkholes that occurred in distance intervals 19 through 21 (4500–5250ft) also greatly exceeded the expected values. Sinkhole occurrence returned to a relatively expected rate at distance interval 22.

Deviations from the surface stream regression model suggested that sinkhole occurrence increases at several hundred feet away from the surface streams and then begins to decline (Table 12, Figure 17). The scatter plot (Figure 17) shows considerable deviation from the predicted values until distance interval 15 (375ft). In the areas nearest the streams (distance intervals 1–3, 0–75 ft), considerably fewer sinkholes occurred compared to the predicted values. In contrast, sinkhole occurrence dwarfed the predicted values in areas between 125–175 ft (distance intervals 6 and 7) from streams. The model also under predicted sinkholes in distance interval 10 (225–250 ft).

Criteria weighting and susceptibility indices

Ranks assigned to the inter-attributes of the criteria were based on the results of the statistical analyses and Hack's (1965) report on the geomorphology of the Shenandoah Valley (Tables 13, 14, and 15). The intra-attribute weights were assigned as follows: the bedrock layer accounts for 50% of the final index; the distance to fault line data layer accounts for 25%; and the distance to surface stream layer accounts for 25%. The varied percentages are attributable to the confidence levels of the models and how well the data conform to theories in the literature. The results of the weighted overlay analysis were classified using natural breaks into low (2-3), moderate (3-4), high (4-5), and very high (5-7) sinkhole susceptibility categories (Table 16, Figure 18).

DISCUSSION

Geologic bedrock

The findings of this study agree with much of the karst literature, which has found that the variation in sinkhole distribution is highly dependent on bedrock type. Of the 13 bedrock classes in our study area, six formations contain sinkholes including the Beekmantown, Conococheague, Edinburg/Oranda, Lincolnshire, New Market Limestone, and Stonehenge (Table 17). With the exception of the Conococheague formation, which formed during the Cambrian period, all of these carbonate formations are of the Ordovician age, and all are composed of limestone and/or dolomite.

Only one limestone/dolomite formation, the Elbrook, did not contain sinkholes. The Elbrook formation is composed of bluish-gray limestone and shaly dolomite, however it differs from most of the other limestone and/or dolomitic rocks in that it is of Cambrian age. Sinkholes

occurred in all carbonate bedrocks of Ordovician age in the study area, with the exception of two outcrops located in the highlands, the Martinsburg and Oranda formations. The Martinsburg formation is composed of shale, sandstone, siltstone and some sporadic thin limestone beds and it is generally considered more heterogeneous than the other carbonate Ordovician bedrocks in the study area. The Oranda bedrock is a very distinctive unit intermixed with calcareous siltstone and sporadic clayey limestones. The heterogeneity of the Oranda formation, and its very small area probably reduce the likelihood of sinkhole occurrence.

With the exception of the Conococheague formation, all sinkhole containing bedrocks are of the Ordovician age and as expected are predominantly limestone and dolomite (Table 17). The Cambrian age Conococheague formation does contain sinkholes, but relatively few (Tables 7 and 8). Sinkholes were more than twice as likely to occur in the other five sinkhole containing bedrocks as the Conococheague formation (Table 8).

The New Market Limestone formation stands out among the sinkhole-prone formations showing the highest mean sink density value and relative risk ratios. While it displayed high density and risk of sinkholes, percent coverage was comparably low because the sinkholes tend to be small in this formation. The New Market Limestone differs from the other Ordovician carbonate rocks in that it is considered to be purest limestone made up of 98% calcium carbonate (Hack 1965; Young and Rader 1974).

Depth of residual mantle is related to purity of the carbonate rock and may also play a role in sinkhole susceptibility of bedrock. The residual mantle refers to a layer of unconsolidated and weathered mineral materials formed by disintegration of consolidated rocks (Schut 2000). Hack (1965) points out that residual mantle depth is extremely variable throughout the

Shenandoah Valley. Thin residual mantles are characteristic of rocks from the middle Ordovician age. Unlike other bedrocks, such as those from the Cambrian age, Ordovician bedrocks do not typically contain enough impurities to produce a significant amount of residuum. Very little residuum can be observed in the New Market Limestone due to its homogeneity. The Edinburg formation is also known to be lacking in residuum (Hack 1965) due to its uppermost member (the St. Luke), which closely resembles the New Market Limestone in its density and purity (Young and Rader 1974). The carbonate Ordovician formations appear to be highly susceptible to sinkhole occurrence due to their relative purity and thin residuums. On the other hand, more heterogeneous carbonate rocks like that of the Conococheague and Elbrook formations tend to be characterized by a relatively thick residual mantle (Hack 1965) that likely impedes sinkhole formation.

Limestone versus dolomite composition does not appear to inhibit or favor sinkhole occurrence. For example, the Beekmantown is highly dolomitic compared to the other formations, but was found to have high relative risk exceeded only by the New Market Limestone. Sinkhole size was highly variable among and within all bedrock types, and was not useful in differentiating bedrock types.

Soil depth to bedrock

In contrast to several karst studies in the literature, this study found that sinkhole distribution was not related to soil depth to bedrock. This result may be due to highly variable soil depths and inadequate spatial resolution of the soil depth data. Sinkholes were nearly equally abundant at soil depths of 0 and 147 feet, and occurred at depths of 51, 89, and 94 feet. These data provide no evidence of a particular pattern in sinkhole distribution across soil depth.

Higher resolution data provided by fieldwork along with site specific analysis may generate different results.

Proximity to fault lines

The reasonably strong positive relationship between proximity to faults and sinkhole occurrence (R^2=0.60, $p<0.05$) may be related to voids that develop around fault lines. Voids enable relatively greater water transport through the bedrock, thus inducing dissolution of carbonate rocks and leading to sinkhole formations. This relationship was overshadowed however by bedrock type in some areas. The anomalously high sinkhole abundance in distance intervals 19–21 appears to be related to the presence of Ordovician carbonate rocks (Figure 19). Those intervals are closely aligned with the thin strips of land underlain by New Market Limestone, which has the highest average sinkhole risk among bedrock types, and Lincolnshire formations.

A map of the bedrock formations and sinkholes, overlain by the distance to fault intervals (Figure 19), clearly shows that sinkholes tended to form in clusters around fault lines in this region. A group of 14 sinkholes cluster around the four faults that converge in the Stonehenge formation. This clustering pattern may also explain the high sinkhole abundance in the first distance interval. It is also worth noting that there are extensive areas adjacent to fault lines in which sinkholes are noticeably lacking. However, this absence only occurs in regions where the bedrock type is not conducive to sinkhole development. This observation, in conjunction with the anomalously high sinkhole occurrences in distance intervals 19, 20, and 21, suggest that although the presence of fault lines positively influences sinkhole development, its importance is outweighed by bedrock type.

Further research could clarify the relationship between sinkhole development and distance to faults. For example, it may be worthwhile to determine if sinkholes tend to occur or cluster around certain types of fault, such as synclinal or anticlinal.

Proximity to surface streams

In a relationship similar to that found by Hack (1965), this analysis showed that sinkhole tend to increase in abundance at some distance away from surface streams rather than immediately adjacent to them. Sinkhole occurrence increased at around 600–1400 feet away from the surface streams and then declined where surface stream distance exceeded 1500 feet (Table 12, Figure 17). This result approximates the findings of Hack (1965), who suggested that this relationship is likely due the groundwater that circulates at some distance away from the streams beneath the surface. Another theory is that the area 600–1400 feet away from the surfaces streams may reflect a zone where both the water table has been lowered over time and a steep hydraulic gradient is present due to the relatively close proximity of the streams (Campbell, personal communication 2005). On the other hand, Orndorff (personal communication 2005) theorizes that the relationship may be explained by the geography of the local floodplains. He notes that in some areas where the floodplain is very large near the main river, sinkhole development will not occur until relief and bedrock exposure begins and the floodplain ends which may be a significant distance from the river (Orndorff, personal communication 2005).

The interesting pattern found between sinkhole occurrence and distance to surface streams is a reminder that karstic landscapes are very specific to the local conditions of the region. It is possible that the sinkhole pattern found in relation to surface streams may have less to do with the local hydrology and more to do with the landscape morphology at those locations.

For example, the areas 600-1400 feet away from streams may have common slopes that play a role in promoting sinkhole development. Further studies are needed to clarify the relationship found in this study between sinkhole distribution and proximity to surface streams. A better understanding of this phenomenon could lead to increased strength of future sinkhole predictive models.

Sinkhole susceptibility index

The sinkhole susceptibility index (Figure 18) is most heavily dependent on bedrock type. Proximity to geologic fault lines and surface streams are together given equal the importance of bedrock type in the index. The bedrock layer is weighted most heavily for two reasons: (1) the statistical analyses in this study indicated that the variation in sinkhole distribution is highly dependent on bedrock type andd (2) these results are affirmation of Hack's (1965) idea that sinkholes are more abundant in Ordovician rocks. Although there were significant relationships found between sinkhole distribution and the two continuous variables, the sinkhole patterns that relate to distance to faults only persist where there are susceptible bedrock types. The sinkhole patterns that relate to distance to streams require more in depth analysis.

The sinkhole susceptibility index (Figure 18) is an important product resulting from this study. The index reflects not only the results of this study, but also the analysis by Hack (1965) in his report on geomorphology of the Shenandoah Valley. In contrast to Hack's (1965) earlier study, this work employed a GIS to investigate the distribution of sinkholes. GIS and statistical analyses facilitated a quantitative investigation of sinkhole distribution while Hack's analyses of sinkhole patterns were largely observational. Despite different methodologies the two studies drew similar conclusions, which give greater strength to both.

This study provides users with a more detailed karst map (Figure 18) based on a range of categories as opposed to the original 1:250,000 scale karst boundary that simply presence or absence of karst. Classification of a susceptibility range as opposed to using a Boolean classification model allows the user to make more informed decisions and provides more flexibility when making those decisions. For example, rather than simply avoiding all karst areas for implementation of any LID practices, the suitability of individual LID practices can be associated with a particular sinkhole susceptibility index based on the extent of infiltration that is facilitated by the LID technique (Table 18). LID techniques such as rain barrels and cisterns are designed to store rather than infiltrate surface water runoff and therefore these practices are suitable in developed areas of very high sinkhole susceptibility. Infiltration is also not the key purpose for downspout disconnections or curb cuts. Instead, these practices are meant to divert the flow of surface water runoff into vegetated areas and therefore they are suitable for areas of moderate sinkhole susceptibility. Infiltration may take place indirectly, so these practices are not recommended in areas of high or very high sinkhole susceptibility. Other LID techniques such as grass swales, bioretention, and pervious pavements are designed to directly infiltrate surface water runoff at the source and therefore they are only suitable in areas of zero to low sinkhole susceptibility. Clearly, the sinkhole susceptibility index offers greater flexibility for development strategies.

This study also provides repeatable methods for analyzing sinkhole distribution in Virginia. Extending this analysis across the entire Shenandoah Valley would further establish the criteria involved in sinkhole development in this region. Additionally, this report enables a comparison between sinkhole distribution patterns of the Shenandoah Valley and other regions. If sinkhole distribution patterns found in this analysis are similar to those found in other regions

where more efforts have been made to protect karst areas, then there is potential for those karst water protection efforts to be applied to karst areas of the Shenandoah Valley region.

There are still inaccuracies and limitations associated with the sinkhole susceptibility index presented here that need to be addressed. For example, the map assumes that sinkhole distribution reflects the pattern of all karst formations. Extensive field work would be required to determine whether caves, springs, and other karst formations of the Shenandoah Valley tend to occur in the same spatial patterns as sinkholes. Uncertainty in the input layers also limits the accuracy of the final map. Hubbard (2004) postulated that there were likely many more sinkholes in the area that he was not able to identify using remote sensing methods. Boundaries associated with the bedrock and faults layer are also probably less than accurate due to the lower resolution techniques available to the original mapping projects, and possible human error during digitization and geo-referencing of the data. A comprehensive evaluation of the uncertainty in the input layers may prove to be a valuable next step.

CONCLUSION AND APPLICATIONS

This analysis used geospatial techniques to determine the relationship between sinkhole distribution and four major landscape factors: bedrock type, soil depth to bedrock, proximity to geologic faults, and proximity to surface streams. The analysis identified three major trends in sinkhole occurrence: (1) sinkholes are more abundant in carbonate rocks of Ordivician age due to their homogeneity and thin residual mantles; (2) sinkhole occurrence increases with proximity to fault lines; and (3) sinkholes are rare near streams, most abundant 600–1400 feet away from surface streams, and decline thereafter with distance. Sinkhole size did not depend upon bedrock types. Neither soil depth to bedrock, nor the type of carbonate rock (limestone or dolomite) were

helpful in distinguishing sinkhole patterns. A sinkhole susceptibility index for the study area was produced based on these findings using weighted overlay analysis in ArcGIS.

The complexity of karst networks in the NSV and the extensive time required to field map karst terrain make verification of the accuracy of this susceptibility index a daunting task. On the other hand, a developing region like the Shenandoah Valley could greatly benefit from such an analysis. Perhaps this study can serve as motivation to continue further research in the arena of karst in the Shenandoah Valley.

Implications for LID site suitability

Adoption of stormwater management design strategies such as LID was an attractive idea to communities of the NSV region because it leads the way in their efforts to thwart the oncoming environmental issues that coincide with urbanization. Unfortunately, the karst terrain that underlies much of the Shenandoah Valley not only compromises urban development, but sustainable development as well. Karst terrain clearly did not impede developers or planners in the past from establishing urban infrastructure as evidenced by Interstate 81 and the metropolitan city of Winchester. This study will help to inform the citizens of the NSV region about the environment they live in. This study has identified key landscape factors and environmental conditions in this region that promote sinkhole development. Use of the sinkhole susceptibility index as a predictive tool in LID site suitability will provide assurance that the stormwater management practices implemented will be more effective.

Recommendations for future work

Launching an expansive field investigation of karst morphology in the Shenandoah Valley would help to clarify sinkhole susceptibility, but would be expensive and time consuming. However, there are other data analyses that were not initiated in this study due to time and financial constraints, which may enhance the robustness of the sinkhole susceptibility model. For example, this study established that carbonate Ordovician age bedrocks are the primary control in facilitating sinkhole development. With this information we could use an alternative approach to analyzing the other criteria, distance from fault lines and distance to surface streams, in a way that produces more definitive conclusions about sinkhole distribution outside of its dependence on bedrock type. Rather than developing individual susceptibility maps for each criteria, weighting them, and adding them together, it may be informative to first extract the carbonate Ordovician rocks from the study area and then use linear regression analysis to estimate the relationship between faults, streams, and sinkhole patterns only within that area. This alternative approach would likely result in higher R^2 values and therefore warrant higher intra-attribute weights for the fault and stream distance layers, reflecting greater accuracy of the sinkhole susceptibility on the ground.

This study also indicates that further analyses are needed to understand the relationship between sinkhole distribution and surface stream hydrology. Presently, most models of hydrological concepts, such as infiltration and surface water runoff, do not consider the presence of karst. Future work should attempt to adjust hydrological models to account for the presence of sinkholes and determine if sinkhole location can be related to infiltration or surface water runoff rates.

Another recommendation for future work is to repeat the methods in this study with higher resolution data. For example, the current soil data available through the SSURGO database is simply not detailed enough to identify the highly variable soil patterns of the NSV region. Higher resolution data, acquired through field or remote methods, could greatly enhance the sinkhole susceptibility model. Likewise, higher resolution elevation data, such as Light Detection and Ranging (LiDAR) data could provide very detailed information about the morphology of the landscape surface, including the shapes and sizes of sinkhole depressions, landscape slope, and vegetation characteristics. LiDAR may also provide information about the underground surface such as the presence of aquifers or sinking streams.

This thesis represents only the beginning of karst research that could be conceived of and useful in the Shenandoah Valley region of Virginia. The use of modern landscape analysis techniques, such as GIS, LiDAR and other remote sensing tools, shows excellent promise for improving karst susceptibility mapping.

LITERATURE CITED

Agresti, A. *An Introduction to Categorical Data Analysis*: John Wiley & Sons, Inc., New York, New York (1996).

Bates, Robert L. and J. A. Jackson. *Glossary of Geology* (Third Edition): American Geological Institute, Alexandria, Virginia, (1987).

Brezinski, D. K., Reger, J. P., and G. R. Baum. "Geologic mapping as a basis for sinkhole susceptibility prediction, Frederick Valley Maryland." Maryland Geological Survey, Environmental Geology & Mineral Resources Online Publications (2003).

Chen, K., Blong, R., and C. Jacobson. "MCE-RISK: integrating multicriteria evaluation and GIS for risk decision–making in natural hazards." Environmental Modeling and Software, 16 (2001):387–397.

Currens, J. C. "Changes in groundwater quality in a conduit-flow-dominated karst aquifer, following BMP implementation." Environmental Geology 42 (2002):525–531.

Denizman, C. "Morphometric and spatial distribution parameters of karstic depressions, lower Suwanee River basin, Florida." Journal of Cave and Karst Studies, 65.1 (April 2003):29–35.

Gao, Yongli, Alexander, E. C. Jr., and R. G. Tipping. "The development of a karst feature database for southeastern Minnesota." Journal of Cave and Karst Studies, 64.1 (April 2002):51–57.

Green, J. A., Marken, W. J., Alexander, E. C. Jr., and S. C. Alexander. "Karst unit mapping using geographic information system technology, Mower County, Minnesota, USA." Environmental Geology, 42 (2002):457–461.

Hack, J. T. "Geomorphology of the Shenandoah Valley, Virginia and West Virginia, and origin of the residual ore deposits: U.S. Geology Survey Professional Paper 484, (1965).

Hubbard, D. A. "Sinkhole Distribution in the central and northern Valley and Ridge province": in Beck, B.F., ed., Sinkholes: Their Geology, Engineering & Environmental Impact, Proceedings of the First Multidisciplinary Conference on Sinkholes, Orlando, FL A.A. Balkema, Rotterdam, (1984): 281–284.

Hubbard, D. A. "Sinkhole Distribution of the Valley and Ridge Province, Virginia." Geotechnical and Environmental Applications of Karst Geology and Hydrology, (April 2001): 33–36.

Hubbard, D. A. "Use of Regional Sinkhole Mapping for Sinkhole Susceptibility

Maps." Sinkholes and the Engineering and Environmental Impacts of Karst, Geotechnical Special Publication No. 122, (September 6–10, 2003): 61–71.

Kastning, E.t H., and K. M. Kastning. "Buffer Zones in Karst Terranes." Karst-Water Environment Symposium Proceedings, Virginia Water Resources Research Center, Virginia Tech, Blacksburg, VA, (1997): 80–87.

Langer, W. H. "Potential environmental impacts of quarrying stone in karst—a literature review." U.S. Geological Survey Open-File Report 0F-01-0484, (2001).

Orndorff, R. C., and G. E. Harlow. "Hydrogeologic Framework of the Northern Shenandoah Valley Carbonate Aquifer System." U.S. Geological Survey Karst Interest Group Proceedings, Shepherstown, West Virginia, (2002).

Rader, E. K., and T. H. Biggs. "Geology of the Strasburg and Toms Brook quadrangles, Virginia." Virginia Division of Mineral Resources Rept. Inv. 45, (1976).

Schut, P. (2000). Retrieved on May 4, 2005 from the internet: http://sis.agr.gc.ca/cansis/intro.html

Shofner, G. A., and H. H. Mills. "A simple map index of karstification and its relationship to sinkhole and cave distribution in Tennessee." Journal of Cave and Karst Studies, 63.2 (April 2001):67–75.

Sokal, R. R., and F. J. Rohlf. *Biometry* (Third Edition): W. H. Freeman and Company (1995).

Stephenson, J. Brad, Zhou, W. F., Beck, B. F., and T. S. Green. "Highway stormwater runoff in karst areas—preliminary results of baseline monitoring and design of a treatment system for a sinkhole in Knoxville, Tennessee." Engineering Geology, 52 (1999):51–59.

Stone, D., and G. M. Schindel. "The application of GIS in support of land acquisition for the protection of sensitive groundwater recharge properties in the Edwards Aquifer of south-central Texas." Journal of Cave and Karst Studies, 64.1 (2002):38–44.

Upton, J. G. *The Analysis of Cross-tabulated Data*: John Wiley & Sons Ltd., Chichester, New York, Brisbane, and Toronto (1978)

Veni, G.. "A Geomorphological Strategy for Conducting Environmental Impact Assessments in Karst Areas." Geomorphology 31 (1999):151–180.

Waltham, A. C., and P. G. Fookes. "Engineering classification of karst ground conditions." Quarterly Journal of Engineering Geology and Hydrogeology, 36 (2003):101–118.

Young, R.S. and E. Rader. "Geology of the Woodstock, Wolf Gap, Conicville, and

Edinburg quadrangles, Virginia." Virginia Division of Mineral Resources Rept. Inv. 35, (1974).

Zwahlen, F., and N. Doerfliger. "Outlining of Protection Areas in Karstic Environment, A New Approach." Karst-Water Environment Symposium Proceedings, Virginia Water Resources Research Center, Virginia Tech, Blacksburg, VA, (1997):54–62.

TABLES

Table 1. LID practices by mapping category. Each category requires an individual LID site suitability map.

Infiltration Based w/Specific Slope Requirement	Infiltration Based w/No Specific Slope Requirement	Non-Infiltration Based
vegetative swale	bio-retention	rain barrels
buffer strip	bio-filter	cisterns
	seepage pits	downspout disconnections
	pervious pavement	reduced road widths
	Infiltration trenches	curb and gutter elimination
		curb cuts
		green roofs

Return to text.

Table 2. Data sources for a sinkhole susceptibility index for a sub-watershed of Shenandoah County, VA.

Type	Scale	Source	Specifications
Karst boundaries	1:250,000	Hubbard, 1983 (DMME)	Based on the identification of sinkholes through stereoscopic viewing of panchromatic aerial photography, and the presence of carbonate rock.
Sinkholes	1:24,000	Hubbard, 1984 (DMME)	Steps for creating this GIS data layer are outlined in Figure 5.
Bedrock and fault lines	1:24,000	Young and Rader, 1974 (DMME), and Rader and Biggs 1976 (DMME)	See text.
Soil depth to bedrock	1:24,000	NRCS	Derived from the Soil Survey Geographic (SSURGO) database acquired from the U.S. Department of Agriculture (USDA), Natural Resources Conservation Service (NCRS).
Surface streams	10 meter	www.mapmart.com	Derived from a digital elevation model (DEM).

Return to text.

Table 3. Geologic bedrock of a sub-watershed in Shenandoah County, VA and its characteristics (adapted from Rader and Young 1974). ABB = abbreviated name of bedrock formations, which will be used throughout this thesis.

AGE	NAME	ABB.	CHARACTER
Devonian	Devonian Rocks	DS	Rock outcrop
Silurian	Tuscarora	Stu	Uniform; resistant to weathering; thick bedded, white ortho-quartzite with a basal conglomerate; red, green, and purple shale.
	Silurian Rocks	Su	Rock outcrop
Ordovician	Martinsburg	Omb	Homogeneous sequence of thick-bedded, peg-weathering, gray, silty shales; sporadic thin beds of limestone.
	Oranda	Oo	Calcereous siltstone resistant to weathering; with intercalated clayey limestones.
	Edinburg	Ooe	Comprises the Lantz Mills and Liberty Hall, and the St. Luke Member; Lantz Mills is thin-bedded, medium grained, dark-gray limestone; Liberty Hall consists of black, thin-bedded shale and dense, black, medium-bedded limestone; St. Luke Member is found only at the top, is pure, dove-gray, fine-grained limestone, close to New Market Limestone.
	Lincolnshire	Ol	Medium to thick-bedded, dark-gray, medium-grained limestone; normally contains nodules of black chert.
	New Market Limestone	On	Contains two units: (1) a lower series of thin-bedded, shaly and dolomitic, buff limestones and carbonate pebble conglomerates; (2) an upper series of massive, dove-gay sublithographic limestones and carbonate pebble conglomerates; upper division is the "quarry limestone" of the Shenandoah Valley and often contains 98% calcium carbonate.
	Beekmantown	Ob	This formation refers to the strata overlying the distinctive, cephalopod-bearing Stonehenge and underlying the sublithographic New Market Limestone; masive to thick-bedded, gray to brown dolomite and variable amounts of white chert; also overlain by Lincolnshire.
	Stonehenge	Ost	Uniformly thick-bedded, bluish-gray, fine to medium grained limestone; nonlaminated in contrast to underlying Conocheague; nondolomitic in contrast with overlying Beekmantown.
	Ordovician Rocks	Ou	Rock outcrop

Table 3. Continued.

AGE	NAME	ABB.	DESCRIPTION
Cambrian	Conococheague	Cco	Most heterogeneous; includes limestones, dolomites, sandstones, silty shales; limestones are rudely laminated and bluish-gray; dolomites are massive, gray, medium-grained.
	Elbrook	Ce	Thick-bedded, non-laminated, bluish-gray limestone and shaly dolomite.

Return to text.

Table 4. Methods for determining sinkhole susceptibility rankings for bedrock types. All criteria are multiplied by the corresponding % influence and summed together to equal the sinkhole susceptibility ranking for the individual bedrock type.

CRITERIA	Ordovician (age)	Carbonate (composition)	Purity/ Residuum	Mean Relative Risk	Sink Density Mean Rank	Percent Coverage Mean Rank	Presence of Sinkholes
% INFLUENCE	[boolean variable] x(10%)	[boolean variable] x(15%)	x(10%)	x(20%)	x(20%)	x(20%)	[boolean variable] x(5%)

Return to text.

Table 5. Chi-square results of Kruskal-Wallis test on bedrock type. Degrees of freedom (df) equal the number of classes of the independent variables minus one. The critical value for $\alpha = 0.05$ with df = 5 is 11.07.

	Percent Sinkhole Coverage	Sinkhole Density (sinks/hectares)	Mean Sinkhole Size (hectares)
Chi-Square	14.0529	13.4542	9.4137
df	5.0000	5.0000	5.0000
Asymp. Sig.	0.0153	0.0195	0.0937

Return to text.

Table 6. The mean ranks produced by the Kruskal-Wallis test showing the relative extent of variation in sinkhole density or percent sinkhole coverage in each bedrock class that contained sinkholes. Ob=Beekmantown, Cco=Conococheaghue, Ost=Stonehenge, On=New Market Limestone, Ol=Lincolnshire, Ooe=Edinburg.

	% Sinkhole Coverage		Sinkhole Density (sinks/hectare)		Average Sinkhole Size (hectares)	
Bedrock Type	N	Mean Rank	N	Mean Rank	N	Mean Rank
Ob	5.00	15.80	5.00	17.00	5.00	16.20
Cco	5.00	3.20	5.00	4.00	5.00	16.80
Ost	5.00	20.00	5.00	16.20	5.00	17.90
On	5.00	14.40	5.00	23.00	5.00	7.80
Ol	5.00	21.80	5.00	19.20	5.00	11.10
Ooe	5.00	17.80	5.00	13.60	5.00	23.20
Total	30.00		30.00		30.00	

Return to text.

Table 7. Results of cross tabulation analysis for bedrock type shown for the five transects that divide the study area. Ob=Beekmantown, Cco=Conococheaghue, Ost=Stonehenge, On=New Market Limestone, Ol=Lincolnshire, Ooe=Edinburg.

Sinkhole Density								
Categories	Low (<0.02)		Moderate (0.02-0.04)		High (0.04-0.07)		Very High (>0.07)	
Bedrock	Count	Percent	Count	Percent	Count	Percent	Count	percent
Ob	0	0	2	25.00	3	42.86	0	0
Cco	5	71.43	0	0	0	0	0	0
Ost	0	0	2	25.00	2	28.57	1	12.50
On	0	0	1	12.50	0	0	4	50.00
Ol	1	14.29	1	12.50	0	0	3.0	37.50
Ooe	1	14.29	2	25.00	2	28.57	0	0
Total	7	100.00	8	100.00	7	100.00	8	100.00
Percent Sinkhole Coverage								
Categories	Low (<0.44)		Moderate (0.44-0.75)		High (0.75-1.26)		Very High (>1.26)	
Bedrock	Count	Percent	Count	Percent	Count	Percent	Count	Percent
Ob	0	0	3	37.50	1	14.29	1	12.50
Cco	5	71.43	0	0	0	0	0	0
Ost	0	0	1	12.50	2	28.57	2	25.00
On	2	28.57	1	12.50	1	14.29	3	37.50
Ol	0	0	1	12.50	1	14.29	3	37.50
Ooe	0	0	2	25.00	2	28.57	1	12.50
Total	7	100.00	8	100.00	7	100.00	8	100.00

Return to text.

Table 8. Odds ratio results for sinkhole occurrence in bedrock type. The mean risk is calculated for the risks shown in each row representing a bedrock type. Ob=Beekmantown, Cco=Conococheaghue, Ost=Stonehenge, On=New Market Limestone, Ol=Lincolnshire,

Relative Risk		Sinkhole?	Ob	Cco	Ost	On	Ol	Ooe	**MEAN RISK**
		Yes	226	24	37	7	15	30	
		No	143	81	27	4	13	23	
Sinkhole?	Yes	No							
Ob	226	143		2.68	1.06	0.96	1.14	1.08	1.39
Cco	24	81	0.37		0.40	0.36	0.43	0.40	0.39
Ost	37	27	0.94	2.53		0.91	1.08	1.02	1.30
On	7	4	1.04	2.78	1.10		1.19	1.12	1.45
Ol	15	13	0.87	2.34	0.93	0.84		0.95	1.19
Ooe	30	23	0.92	2.48	0.98	0.89	1.06		1.27

Return to text.

Table 9. Coefficients of the regression line for continuous variables.

Distance to Fault (x250 ft)				
Unstandardized Coefficients	Std. Error	Standardized Coefficients	t	Sig.
24.22	2.29		10.57	0.00
-0.83	0.13	-0.77	-6.46	0.00
Distance to Streams (x100 ft)				
Unstandardized Coefficients	Std. Error	Standardized Coefficients	t	Sig.
27.61	3.22		8.58	0.00
-1.08	0.22	-0.72	-5.0	0.00

Return to text.

Table 10. Results of the ANOVA for the continuous variables.

Distance to Fault	Sum of Squares	df	Mean Square	F	Sig.
Regression	1561.74	1	1561.74	41.70	0.00
Residual	1048.56	28	37.45		
Total	2610.30	29			
Distance to Stream	**Sum of Squares**	**df**	**Mean Square**	**F**	**Sig.**
Regression	1518.48	1	1518.48	24.95	0.00
Residual	1399.68	23	60.86		
Total	2918.16	24			

Return to text.

Table 11. Regression model summaries for continuous variables.

Distance to Fault			
R	R^2	Adjusted R^2	Std. Error of the Estimate
0.77	0.60	0.58	6.12
Distance to Stream			
R	R^2	Adjusted R^2	Std. Error of the Estimate
0.72	0.52	0.50	7.80

Return to text.

Table 12. Sinkhole occurrences and expected occurrences in fault distance intervals and surface stream distance intervals.

Fault Distance Interval (x250 ft)	# of sinks that occurred	% of sinks that occurred	# of expected sinks	Stream Distance Interval (x100 ft)	# of sinks that occurred	% of sinks that occurred	# of expected sinks
1	40	11.8	23.39	1	13	3.83	26.53
2	25	7.37	22.55	2	8	2.36	25.45
3	15	4.42	21.72	3	14	4.13	24.37
4	20	5.9	20.88	4	22	6.49	23.29
5	12	3.54	20.05	5	25	7.37	22.21
6	26	7.67	19.22	6	35	10.32	21.13
7	20	5.9	18.38	7	32	9.44	20.04
8	21	6.19	17.55	8	23	6.78	18.96
9	14	4.13	16.71	9	19	5.6	17.88
10	9	2.65	15.88	10	29	8.55	16.8
11	11	3.24	15.05	11	21	6.19	15.72
12	12	3.54	14.21	12	22	6.49	14.64
13	8	2.36	13.38	13	21	6.19	13.56
14	11	3.25	12.54	14	19	5.6	12.48
15	8	2.36	11.71	15	9	2.65	11.4
16	3	0.88	10.88	16	11	3.24	10.32
17	6	1.77	10.04	17	6	1.77	9.24
18	4	1.18	9.21	18	5	1.47	8.16
19	19	5.6	8.37	19	2	0.59	7.08
20	22	6.49	7.54	20	1	0.29	6.0
21	10	2.95	6.71	21	1	0.29	4.91
22	6	1.77	5.87	22	0	0	3.83
23	8	2.36	5.04	23	1	0.29	2.75
24	5	1.47	4.20	24	0	0	1.67
25	0	0	3.37	25	0	0	0.59
26	0	0	2.54	n/a	n/a	n/a	n/a
27	0	0	1.70	n/a	n/a	n/a	n/a
28	2	0.59	0.87	n/a	n/a	n/a	n/a
29	2	0.59	0.03	n/a	n/a	n/a	n/a
30	0	0	0	n/a	n/a	n/a	n/a

Return to text.

Table 13. Geologic bedrock sinkhole susceptibility rankings based on the sum of individual criteria multiplied by weighting factors.

PERCENT INFLUENCE BEDROCK	10% Ordovician	15% carbonate	10% purity/ residuum	20% mean relative risk	20% mean sink density rank	20% mean % cover rank	5% Sinks?	SUM OF FACTORS	(SUM/MAX RANK)X4	FINAL RANK
Beekmantown	1	1	0.5	1.39	0.74	0.72	1	0.01	3.60	7
Conococheague	0	1	0	0.39	0.17	0.15	1	0.00	1.34	3
Stonehenge	1	1	0.5	1.30	0.70	0.92	1	0.01	3.66	7
Martinsburg	1	0.5	0	0.00	0.00	0.00	0	0.00	0.69	2
Oranda	1	0.5	0	0.00	0.00	0.00	0	0.00	0.69	2
New Market Limestone	1	1	1	1.45	1.00	0.66	1	0.01	4.00	8
Lincolnshire	1	1	0.5	1.19	0.83	1.00	1	0.01	3.74	7
Edinburg/someOranda	1	1	1	1.27	0.59	0.82	1	0.01	3.66	7
Elbrook	0	1	0	0.00	0.00	0.00	0	0.00	0.59	1
Ordovician Rocks	1	0	0	0.00	0.00	0.00	0	0.00	0.39	1
Tuscarora	0	0	0	0.00	0.00	0.00	0	0.00	0.00	NoData
Silurian Rocks	0	0	0	0.00	0.00	0.00	0	0.00	0.00	NoData
LowDevonian/UpSilurian Rocks	0	0	0	0.00	0.00	0.00	0	0.00	0.00	NoData

Return to text.

Table 14. Sinkhole susceptibility rankings for distance from fault intervals.

Proximity to Fault	Rank
Distance Interval 1 (0–250 ft)	8
Intervals 2–5	6
Intervals 6–15 (expected sinks > mean)	4
Intervals 16–24 (expected sinks > 5)	3
Intervals 24–30 (expected sinks < 5)	1

Return to text.

Table 15. Sinkhole susceptibility rankings for distance from stream intervals.

Proximity to Surface Streams	Rank
Intervals 1–3	3
Intervals 4, 11–14	6
Intervals 6–7	8
Intervals 5, 8–10	7
Intervals 15–20	2
Intervals 21–25	1

Return to text.

Table 16. Sinkhole susceptibility index. Values are based on the results of the overlay weighted analysis performed using ArcGIS. The overlay weighted analysis was based on the following equation: bedrock inter-attributes (%50) + fault line distance inter-attributes (%25) + stream distance inter-attributes (%25). The values were classified into four susceptibility categories (low to very high) by natural breaks.

Susceptibility Category	Susceptibility Index value (unitless)
Low	2 – 3
Moderate	3 – 4
High	4 – 5
Very high	5 – 7

Return to text.

Table 17. Attributes of sinkhole containing bedrocks that increase sinkhole susceptibility.

BEDROCK	Ordovician Age	predominantly composed of limestone and/or dolomite	sinkholes present
Beekmantown	x	x	x
Conococheague		x	x
Stonehenge	x	x	x
Martinsburg	x		
Oranda	x		
New Market Limestone	x	x	x
Lincolnshire	x	x	x
Edinburg/someOranda	x	x	x
Elbrook		x	
Ordovician Rocks	x		
Tuscarora			
Silurian Rocks			
LowDevonian/UpSilurian Rocks			

Return to text.

Table 18. Associating LID suitability with sinkhole susceptibility. Suitable sinkhole susceptibility indices (none, low, moderate, high, or very high) are denoted by an "x" for individual LID practices based on infiltration requirements of the practice.

	Sinkhole Susceptibility				
LID Practices	None	Low	Moderate	High	Very High
Grass swale	x	x			
Buffer strip	x	x			
Bioretention	x				
Bio-filter	x				
Seepage pits	x				
Pervious pavement	x	x			
Infiltration trenches	x				
Rain barrels	x	x	x	x	x
Cisterns	x	x	x	x	x
Downspout disconnections	x	x	x		
Reduced road widths	x	x	x		
Curb and gutter elimination	x	x	x		
Curb cuts	x	x	x		
Green roofs	x	x	x	x	x

Return to text.

FIGURES

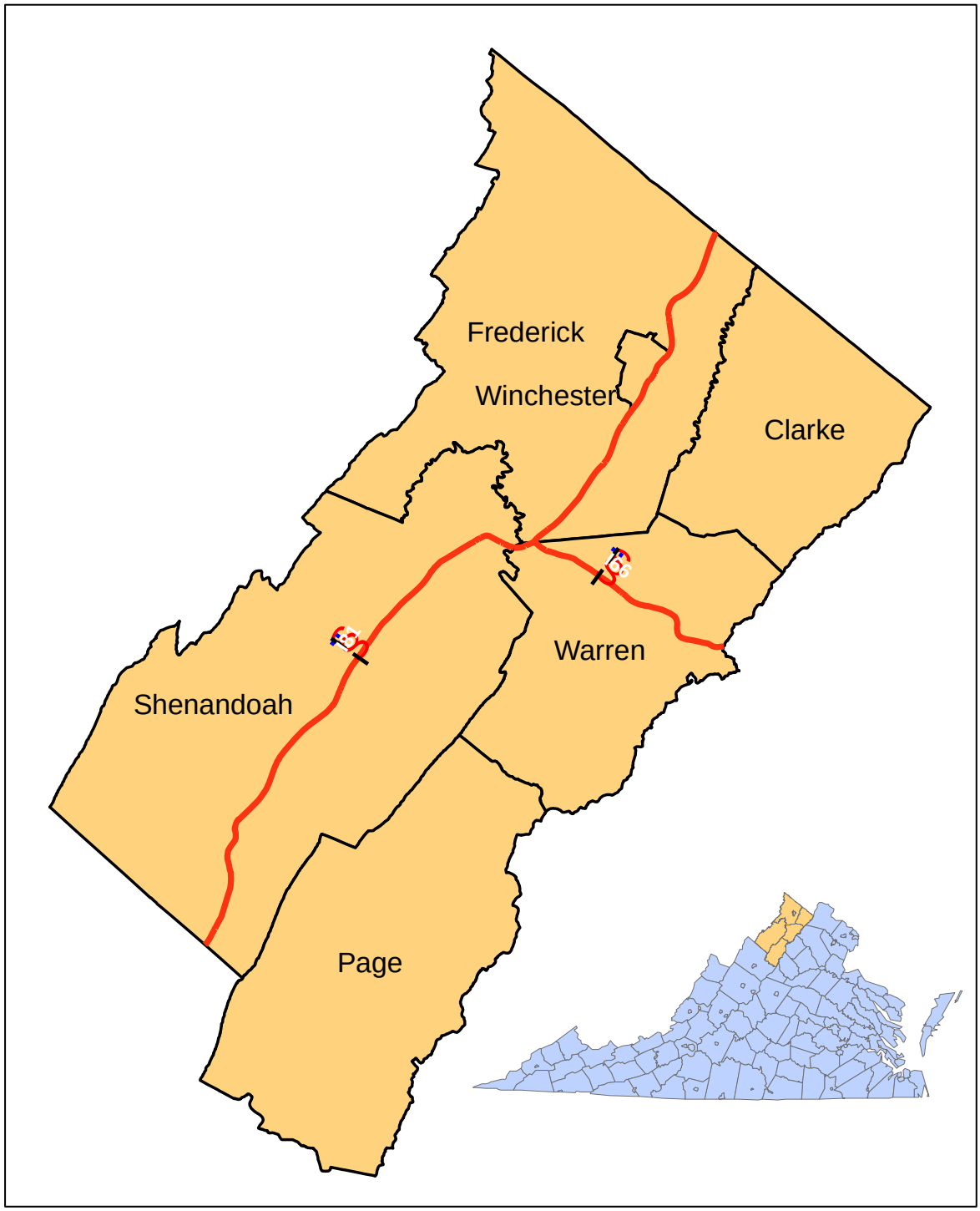

Figure 1. Northern Shenandoah Valley (NSV) region of VA showing counties, cities, Interstate 81, and Interstate 66.

Return to text.

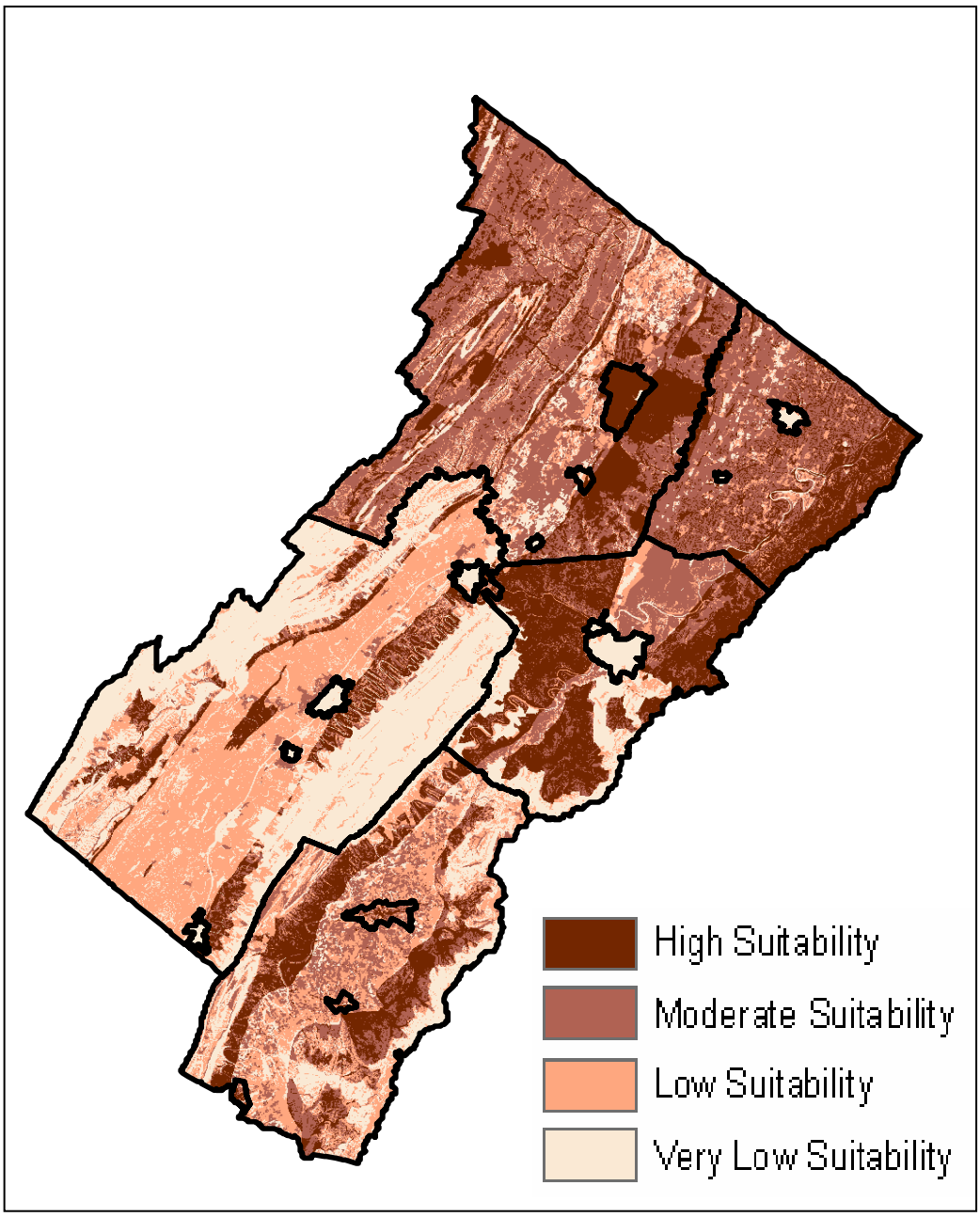

Figure 2. Site suitability map for infiltration based Low Impact Development (LID) practices that require specific slopes for the Northern Shenandoah Valley (NSV) region of Virginia. Produced by the Center for Geospatial Information Technology (CGIT) at Virginia Tech.

Return to text.

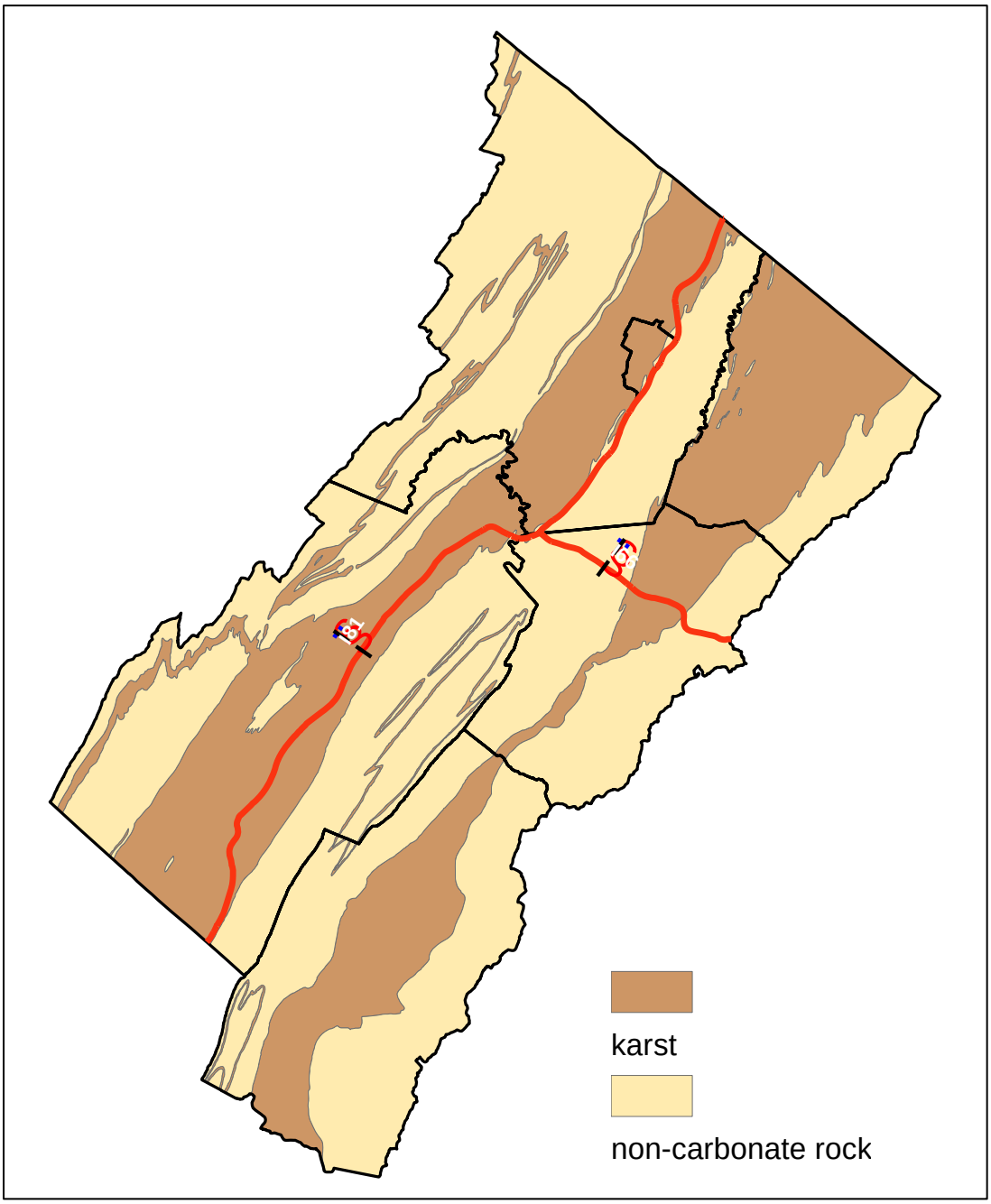

Figure 3. Karst map of the Northern Shenandoah Valley (NSV) region at the 1:250,000 scale. The map was classified using a Boolean classification model: karst = 1, non-carbonate rock = 0. This map was incorporated in the Low Impact Development (LID) site suitability maps with karst ares considered unsuitable for LID and non-carbonate rock areas considered suitable for LID.

Return to text.

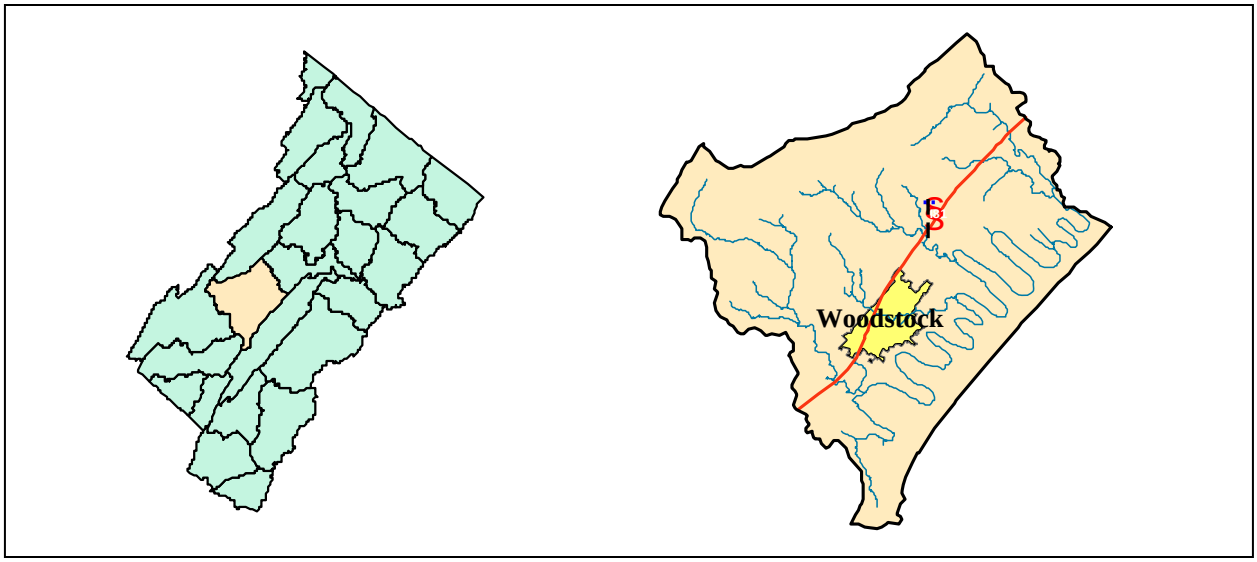

Figure 4. Watersheds of the Northern Shenandoah Valley (NSV) region of Virginia (left) and a sub-watershed of the North Fork Shenandoah watershed (right) that serves as the study area.

Return to text.

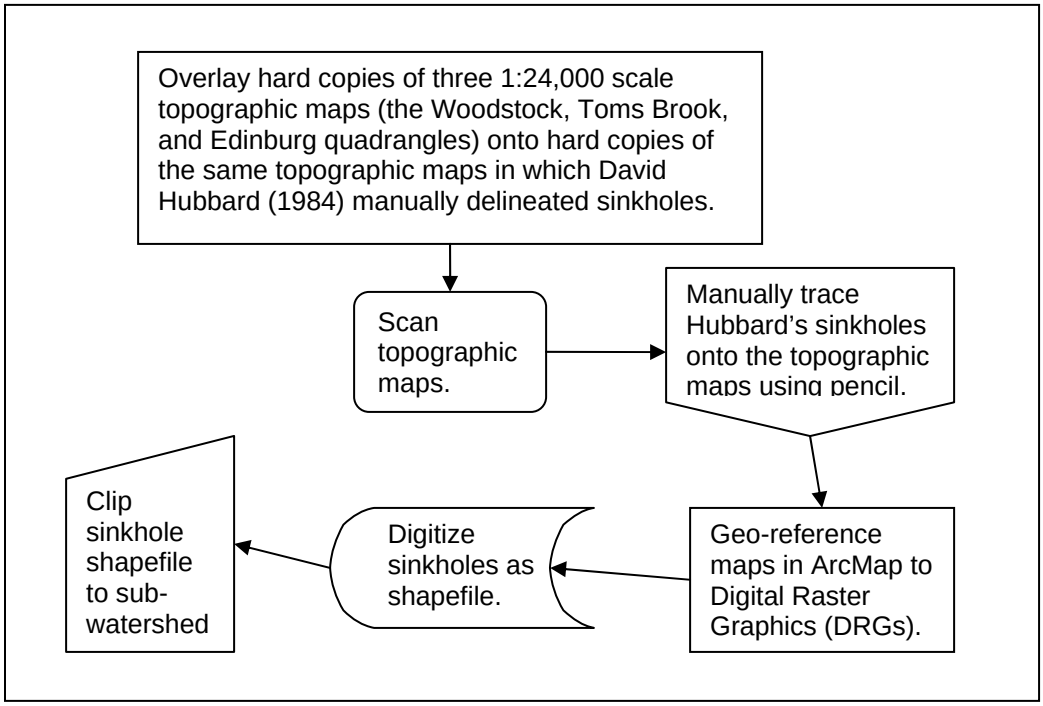

Figure 5. Method for creating a GIS data layer for the 1:24,000 scale sinkholes produced by Geologist Specialist, David Hubbard of the Virginia Department of Mines and Minerals (DMME).

Return to table.

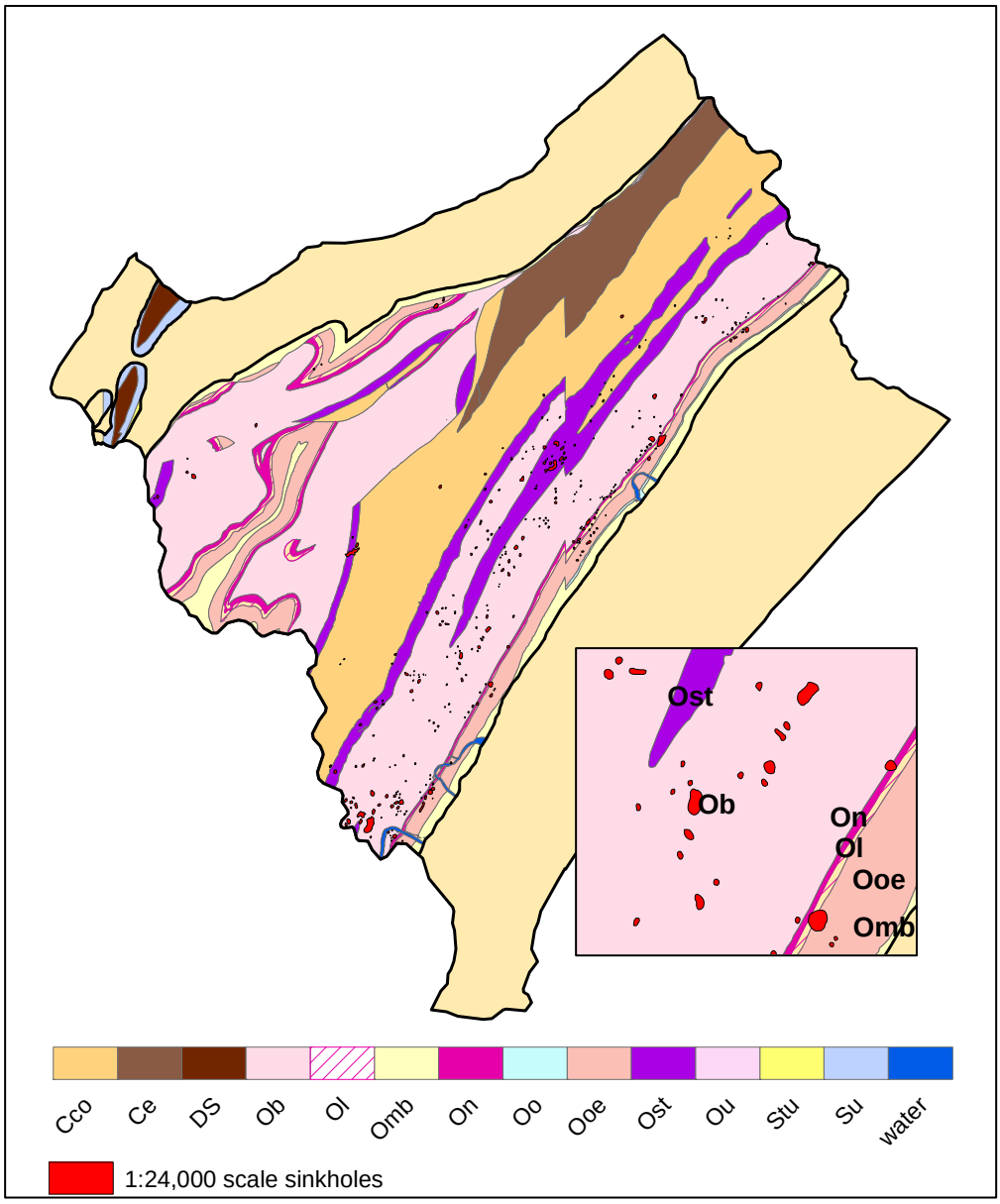

Figure 6. Geologic bedrock layer for carbonate rocks of the study area. Ob=Beekmantown, Cco=Conococheaghue, Ost=Stonehenge, On=New Market Limestone, Ol=Lincolnshire, Ooe=Edinburg. The distinct offset in the bedrock data in the center of the study area represents the boundary between the Woodstock and Toms Brook quadrangles. The different dates, personnel, and methods of mapping between the two quadrangles account for the offset.

Return to text.

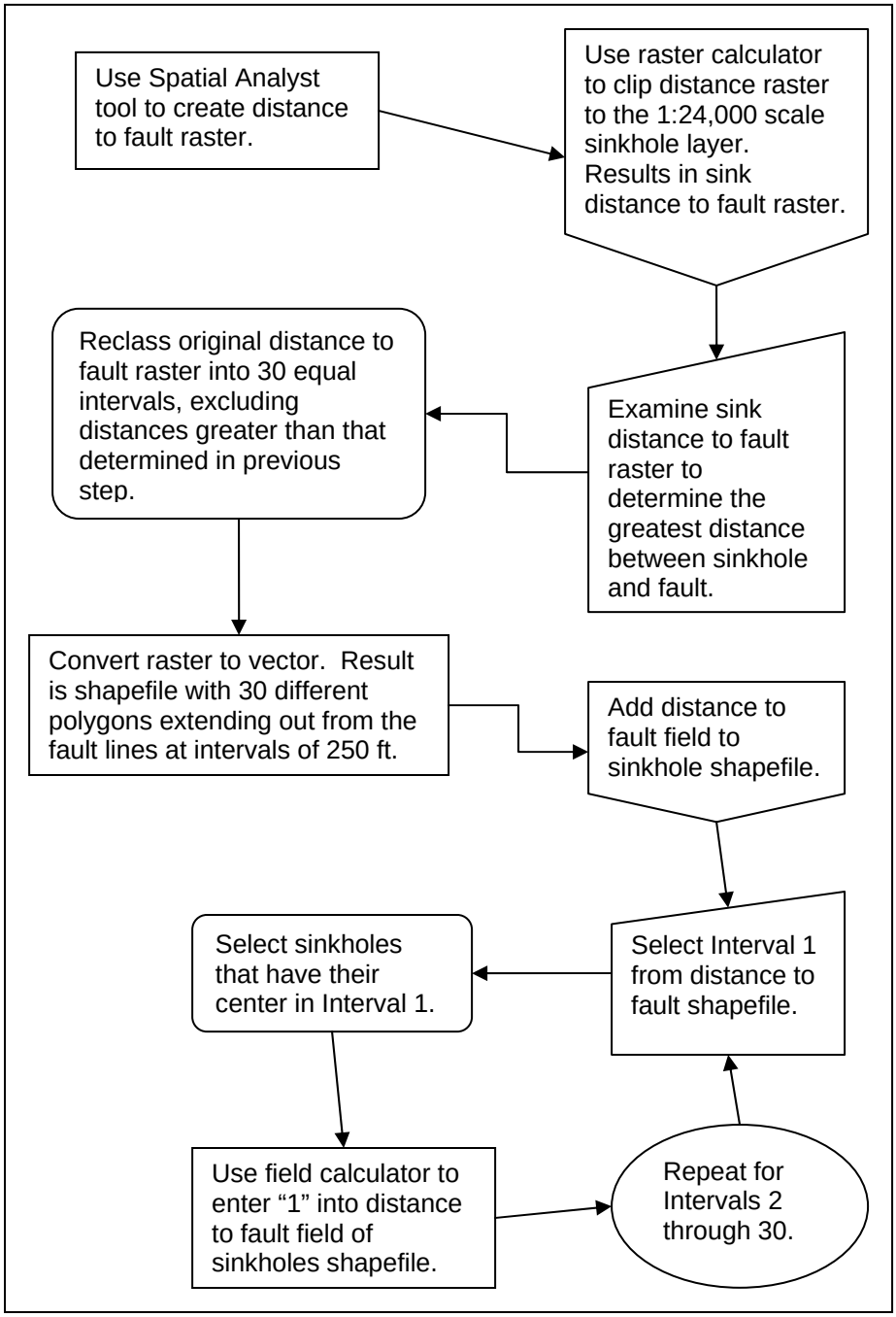

Figure 7. Methods for assigning a distance to fault interval to each sinkhole based on the location of the center of the sinkhole.

Return to text.

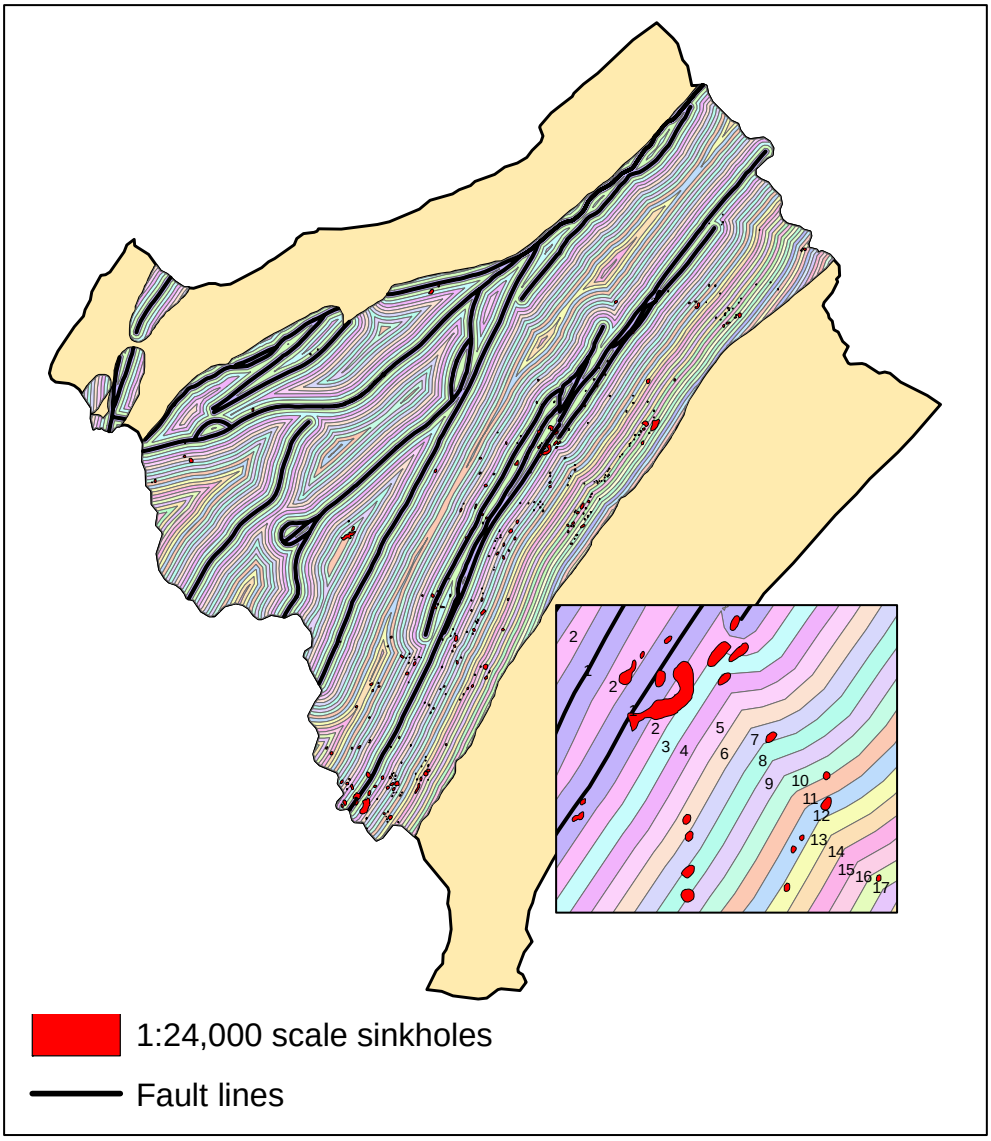

Figure 8. Distance to fault line intervals 1 (0-250 ft) to 30 (7250-7500 ft) for study area. Each distance interval is 250 ft wide.

Return to text.

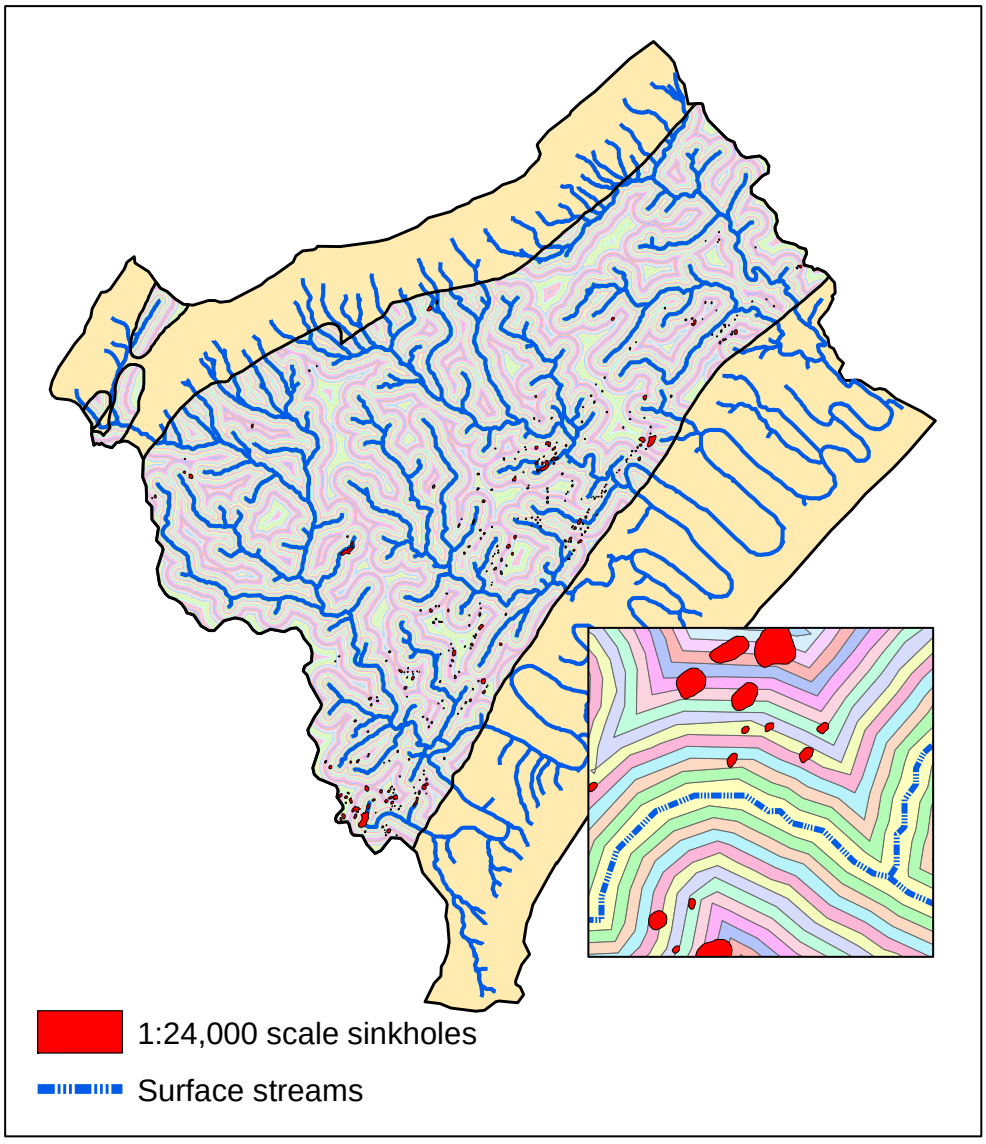

Figure 9. Distance to surface stream intervals 1 (0–100 ft) to 25 (2400–2500 ft) for study area. Inset shows a zoomed in view of the map.

Return to text.

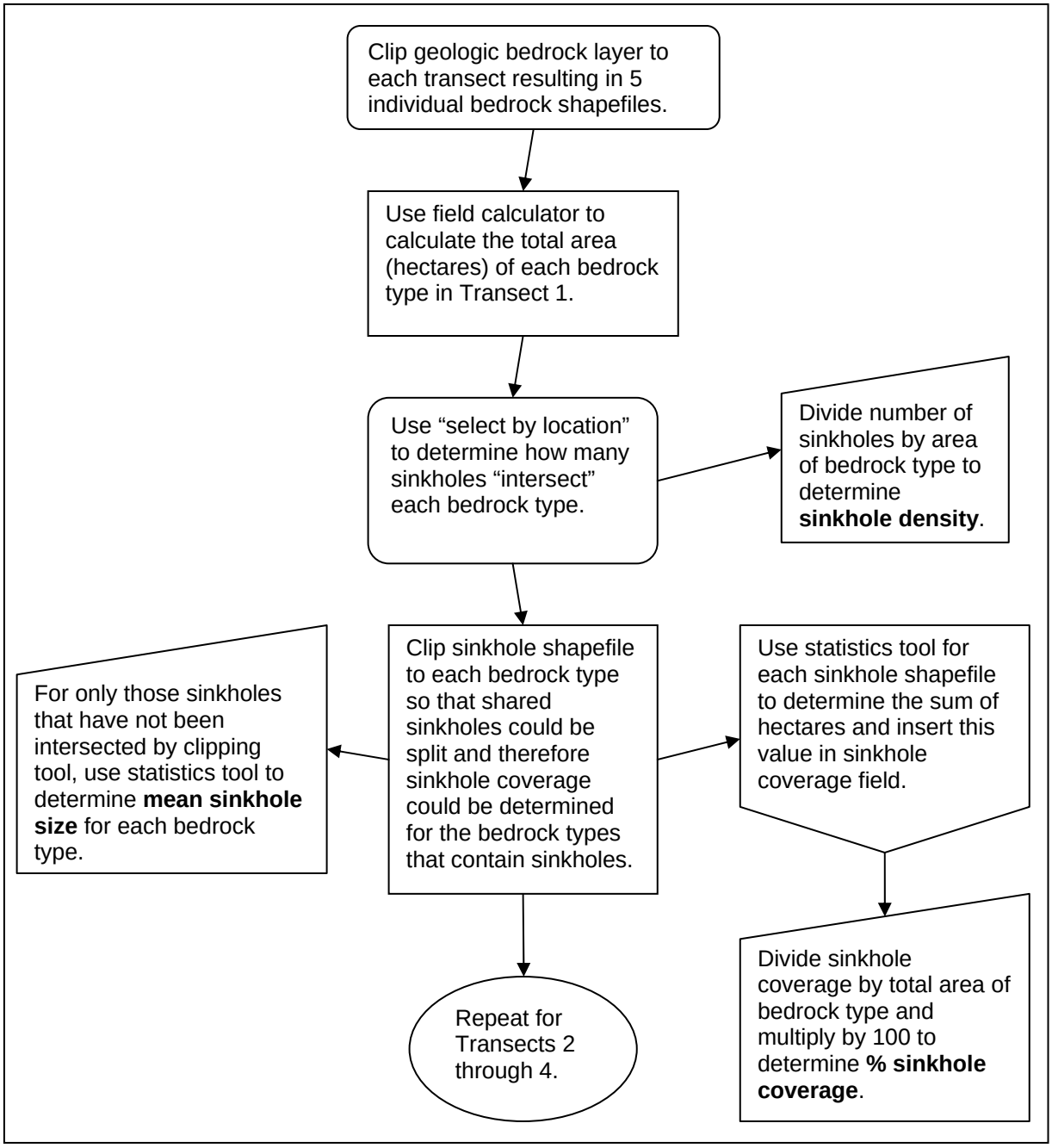

Figure 10. Methods for determining sinkhole density, mean sinkhole size, and % sinkhole coverage for each bedrock type across the five transects.

Return to text.

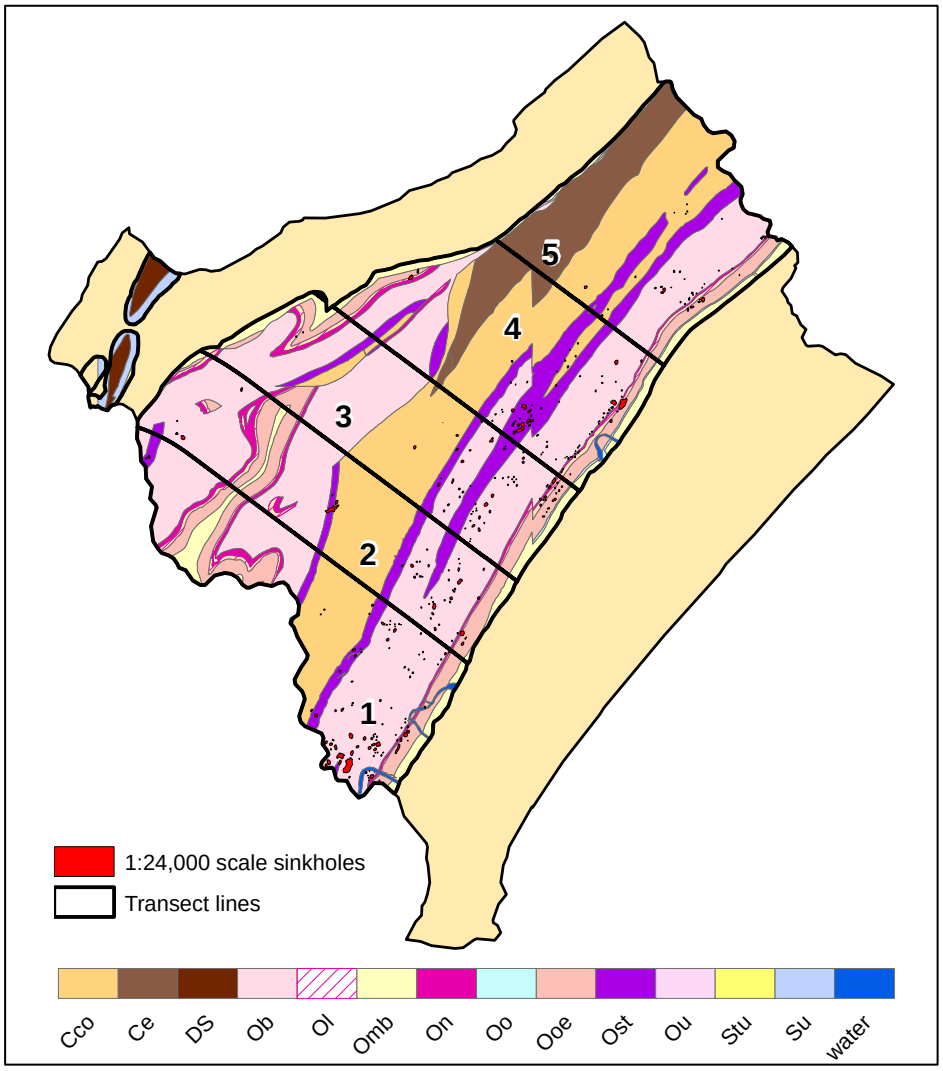

Figure 11. The five transects (approximately equal in area, generated by the GIS) used for comparison of sinkhole distribution using the Kruskal-Wallis statistic . Ob=Beekmantown, Cco=Conococheaghue, Ost=Stonehenge, On=New Market Limestone, Ol=Lincolnshire, Ooe=Edinburg.

Return to text.

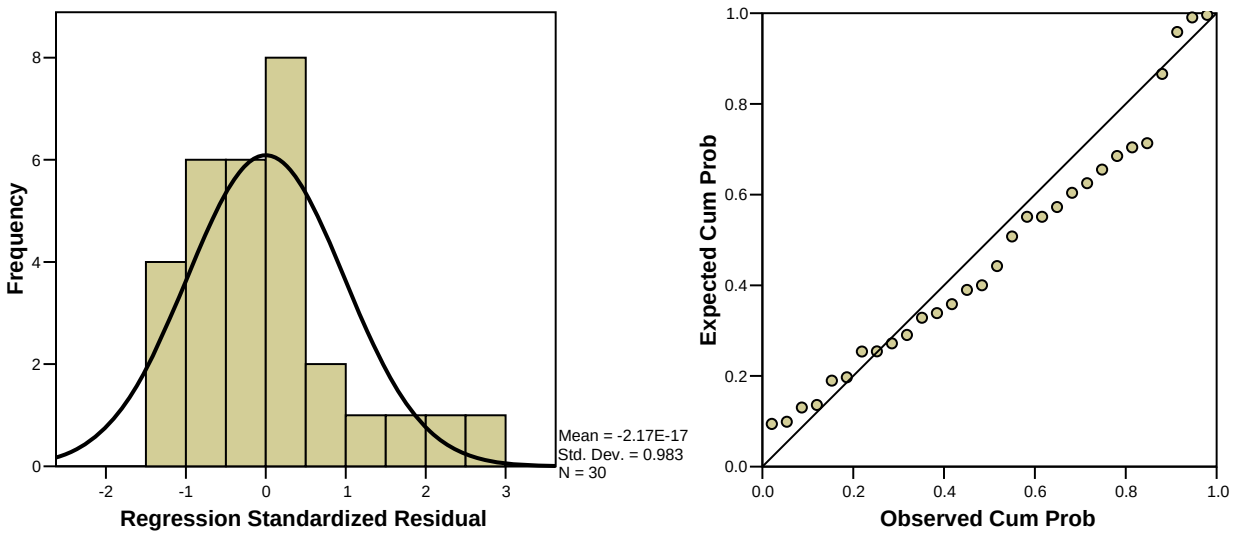

Figure 12. Histogram and P-P plot for distance to fault data. The graphs verify that the distance to fault data were normally distributed. Return to text.

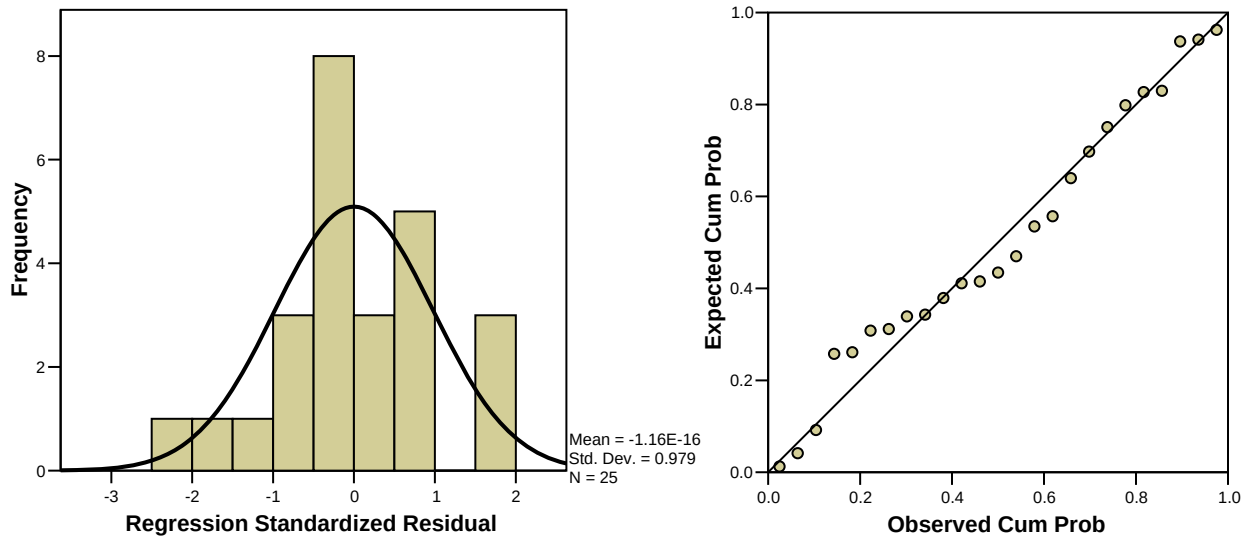

Figure 13. Histogram and P-P plot for distance to surface stream data. The graphs verify that the distance to surface stream data were normally distributed. Return to text.

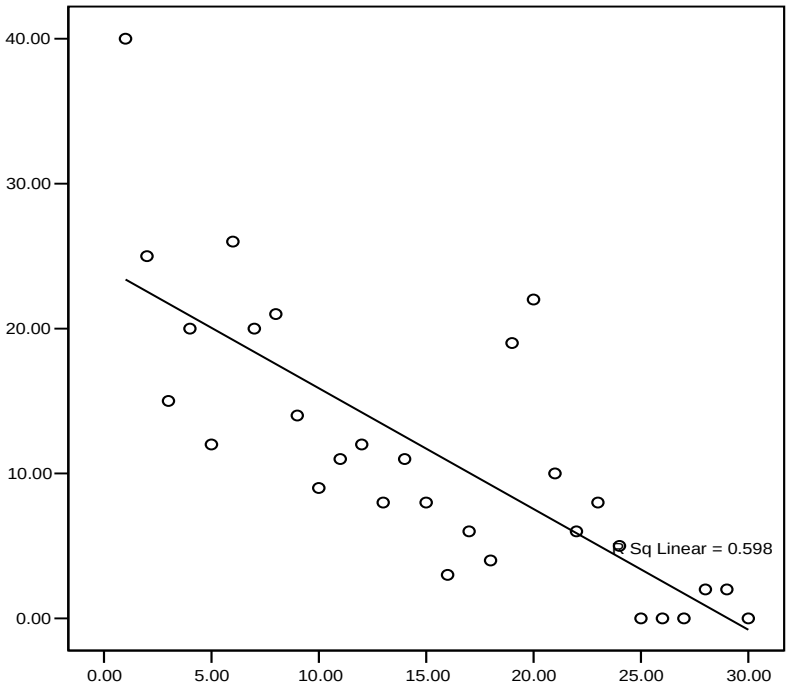

Figure 14. Scatter plot for the number of sinkholes (y axis) versus the distance to fault intervals, 0–30 (0–7500ft) (x axis). Return to text.

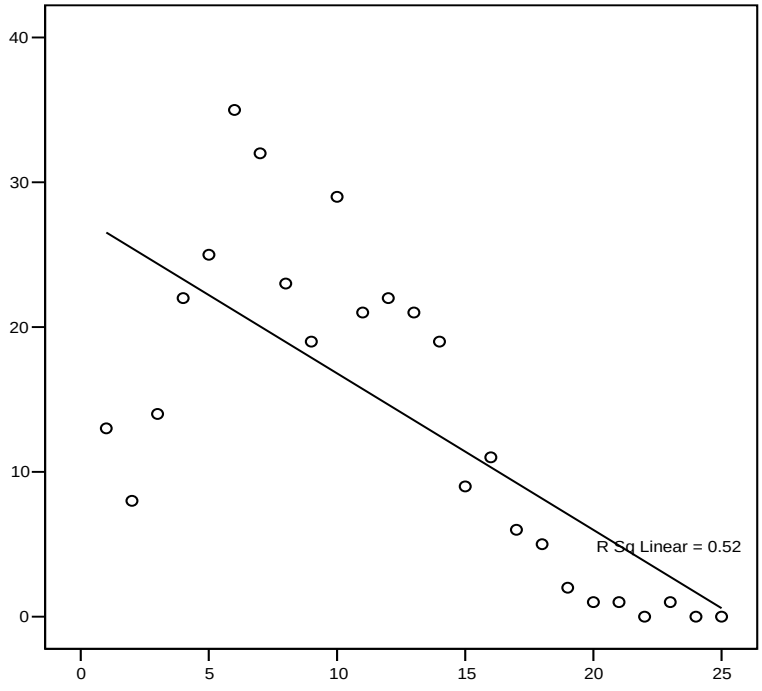

Figure 15. Scatter plot for the number of sinkholes (y axis) versus the distance to surface stream intervals, 0–25 (0–2500ft) (x axis). Return to text.

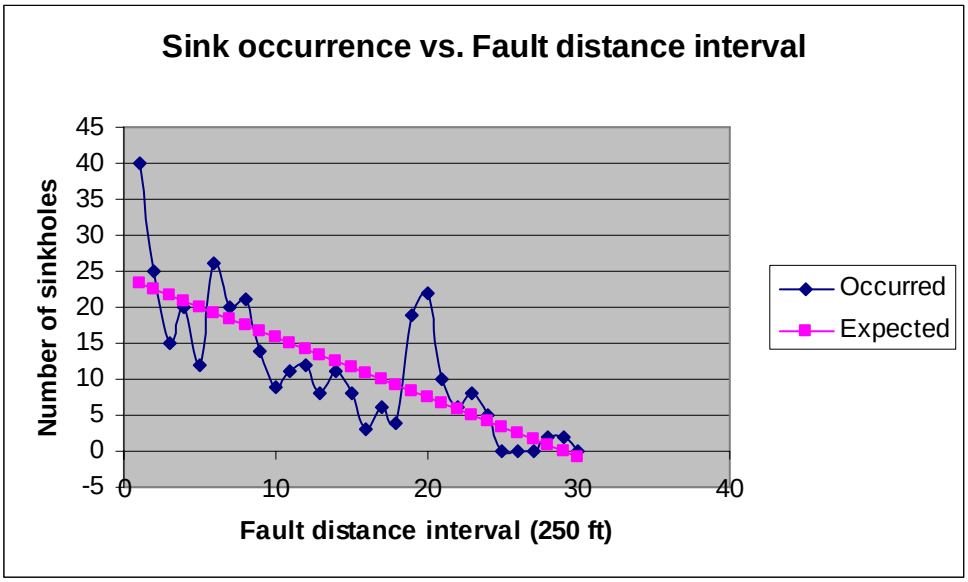

Figure 16. Scatter plots of the number of occurred sinkholes overlaid by scatter plots of the number of expected number sinkholes, as predicted by the regression model. Return to text.

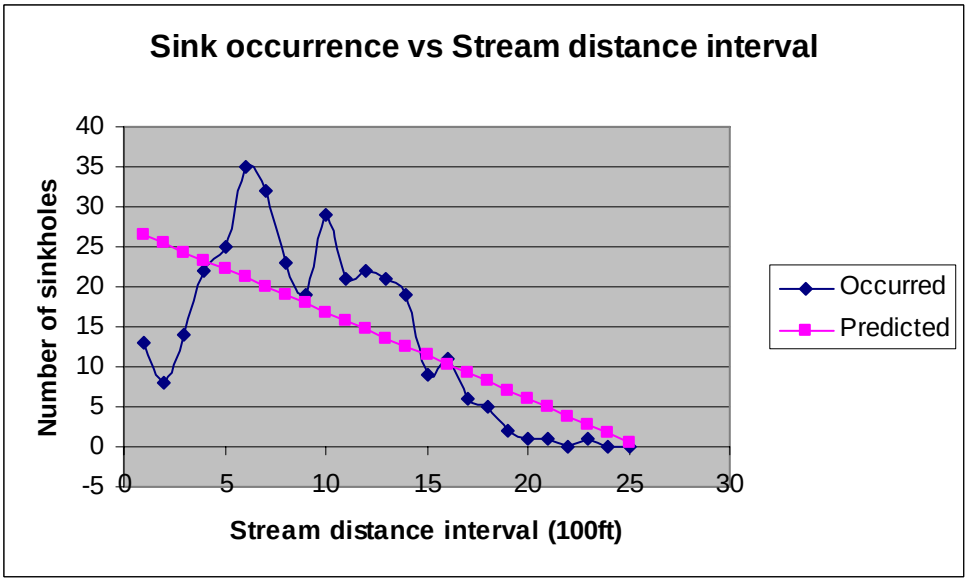

Figure 17. Scatter plots of the number of occurred sinkholes overlaid by scatter plots of the number of expected number sinkholes, as predicted by the regression model. Return to text.

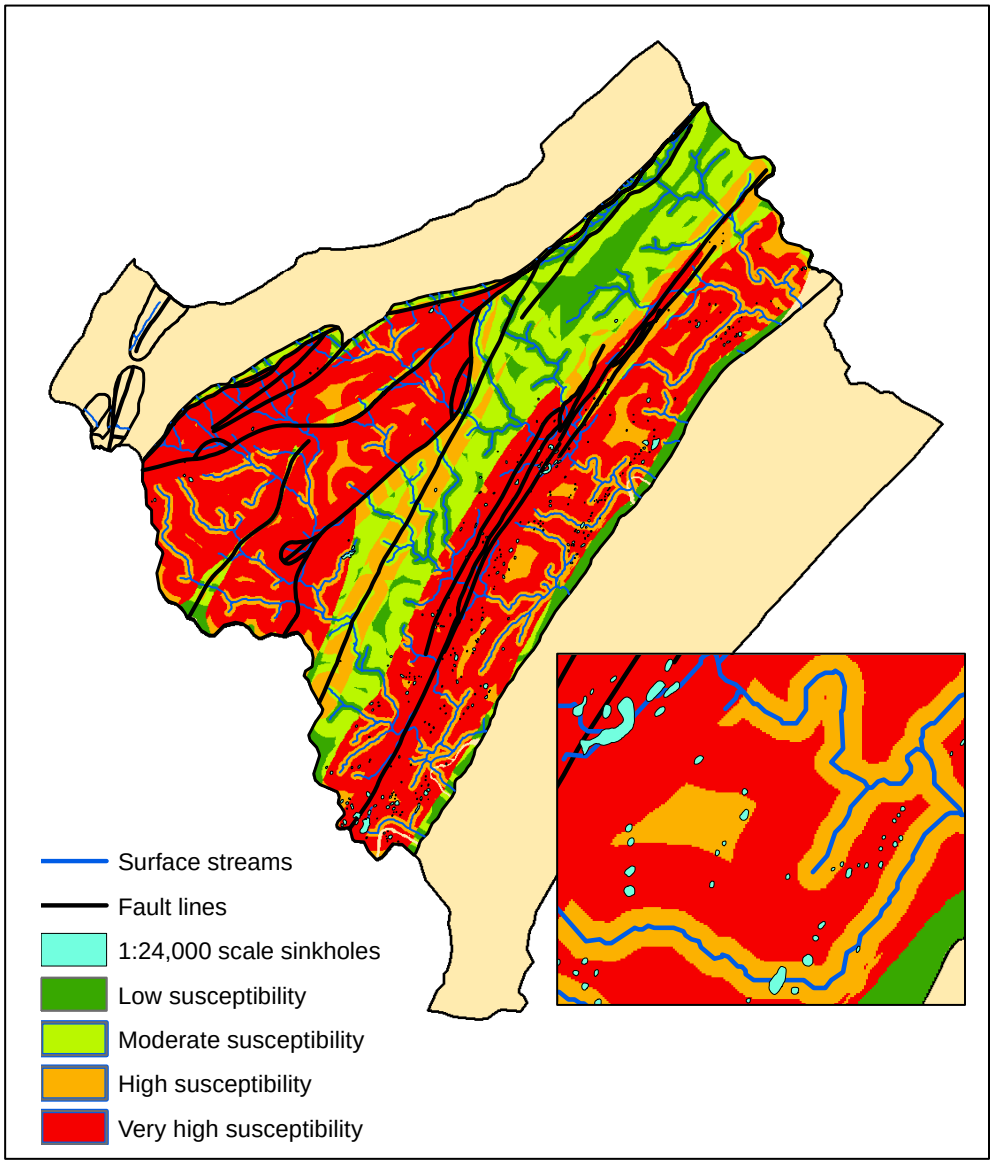

Figure 18. Sinkhole susceptibility index for a sub-watershed of the North Fork Shenandoah watershed of Shenandoah County. The index is based on three criteria that were found to influence the development of sinkholes: (1) bedrock type; (2) distance from fault lines; and (3) distance from surface streams. Return to text.

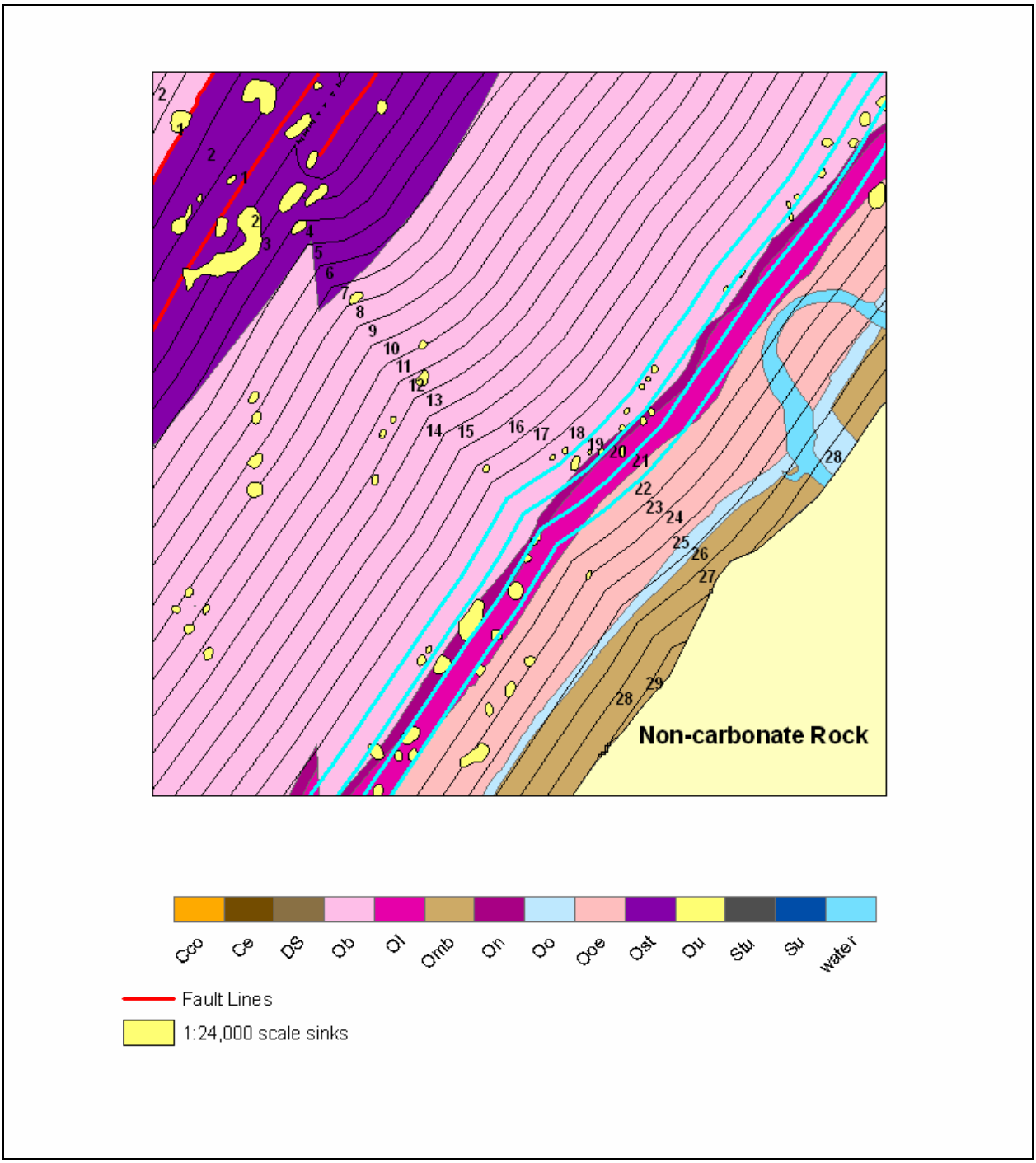

Figure 19. Partial map of study area showing fault distance intervals 19, 20, and 21, which contain more sinkholes than predicted by the regression model. The anomalies occur in intervals closely aligned with the New Market Limestone and Lincolnshire formations, which are highly susceptible to sinkhole occurrence. Ob=Beekmantown, Cco=Conococheaghue, Ost=Stonehenge, On=New Market Limestone, Ol=Lincolnshire, Ooe=Edinburg.

Return to text.